

Silencing of long non-coding RNA CASC15 enhances radiosensitivity of esophageal squamous cell carcinoma through microRNA-140-5p-dependent inhibition of MMP7

Chengliang Yang^{1,*}, Yufeng Ba^{2,*}, Xiaoli Zheng¹, Ke Ye¹, Hong Ge¹, Yanan Sun¹, Yufei Lu¹

¹Department of Radiation Oncology, Affiliated Cancer Hospital of Zhengzhou University (Henan Cancer Hospital), Zhengzhou 450008, P. R. China

²Department of Thoracic Surgery, Affiliated Cancer Hospital of Zhengzhou University (Henan Cancer Hospital), Zhengzhou 450008, P. R. China

*Equal contribution

Correspondence to: Hong Ge; email: gehong5@126.com

Keywords: long non-coding RNA CASC15, microRNA-140-5p, matrix metalloproteinase 7, esophageal squamous cell carcinoma, radiosensitivity

Received: January 8, 2020

Accepted: March 31, 2020

Published:

Copyright: © 2021 Yang et al. This is an open access article distributed under the terms of the [Creative Commons Attribution License](https://creativecommons.org/licenses/by/3.0/) (CC BY 3.0), which permits unrestricted use, distribution, and reproduction in any medium, provided the original author and source are credited.

ABSTRACT

Since radioresistance is a common challenge leading to decreased efficiency of radiotherapy for esophageal squamous cell carcinoma (ESCC), no effective treatment strategy has yet been upheld. The current study aimed to explore whether long non-coding RNAs (lncRNA) cancer susceptibility 15 (CASC15) binding to microRNA-140-5p (miR-140-5p) affects ESCC radiosensitivity. Firstly, up-regulated levels of lncRNA CASC15 were found in ESCC tissues and cells. Next, in order to evaluate the effect of lncRNA CASC15 on ESCC, we performed a series of *in vitro* experiments after transfecting the plasmids into KYSE270 and EC109 cells. Results revealed that lncRNA CASC15 silencing contributed to anti-proliferative, anti-invasive and pro-apoptotic properties in ESCC cells. As validated by dual-luciferase reporter assay, lncRNA CASC15 could competitively bind to miR-140-5p that targeted MMP7. Further examination revealed that MMP7 was highly-expressed while miR-140-5p was poorly expressed in ESCC tissues and cells. Meanwhile, the data obtained from radiosensitivity experimentation demonstrated that lncRNA CASC15 elevation inhibited radiosensitivity and apoptosis, yet increased proliferation by binding to miR-140-5p and up-regulating MMP7. Moreover, silencing lncRNA CASC15 *in vivo* enhanced the radiosensitivity of ESCC cells. Collectively, silencing lncRNA CASC15 enhances radiosensitivity of ESCC through miR-140-5p-dependent inhibition of MMP7, highlighting promising new targets for ESCC treatment.

INTRODUCTION

Esophageal cancer (EC), a severe malignancy of the digestive tract, is accompanied by unsatisfactory prognosis and high mortality rates [1, 2]. Pathologically, EC is classified into two types: esophageal squamous cell carcinoma (ESCC) and esophageal adenocarcinoma, with ESCC representing the predominant type [3, 4]. ESCC pathogenesis is associated with alcohol consumption and cigarette

smoking, and related with marked amplification in morbidity [5]. A significant reason for the high mortality of EC is that the majority of EC patients are diagnosed at advanced stages, rendering proactive therapies useless [6]. Currently, surgical intervention is regarded as the gold standard among the traditional therapeutic avenues for patients with EC diagnosed at an early stage, whereas perioperative chemotherapy or chemoradiotherapy are reserved for patients with EC at locally advanced stages [7–9]. However, the

development of radioresistance is known to serve as therapeutic-blockade, thereby leading to subsequent treatment failures or a more aggressive ESCC phenotype, which poses a major clinical challenge for the treatment of ESCC [10, 11]. Therefore, in-depth investigation on the molecular mechanisms underlying radiosensitivity or radioresistance may ultimately provide an insight and therapeutic target to improve the prognosis and minimize the risk of recurrence in ESCC patients.

Long non-coding RNAs (lncRNAs) are categorized as non-protein-coding transcripts with a length of 200 or longer nucleotides, which possess the ability to play crucial roles in both tumor development and progression [12, 13]. Accumulating evidence has indicated the association of various lncRNAs with the pathogenesis and radiosensitivity of EC [14]. lncRNA cancer susceptibility candidate 15 (lncRNA CASC15), also known as LINC00340, was previously identified as a neuroblastoma susceptibility gene by genome-wide association studies [15]. Yao et al. have demonstrated that lncRNA CASC15 could increase the proliferation of gastric cancer cells, as a risk factor for gastric cancer prognosis [16]. Moreover, lncRNA CASC15 has been reported to accelerate the proliferation, migration, and invasion of hepatocellular carcinoma cells, by functioning as an onco-lncRNA [17]. Considering the involvement of lncRNA CASC15 in the regulation of numerous types of cancers, we speculated whether lncRNA CASC15 could exert promotive effects on the tumorigenesis and progression of ESCC and hence affecting the radiosensitivity of ESCC cells.

An existing research indicated the presence of co-expression networks of lncRNA with microRNA (miRNA) in ESCC [18]. Meanwhile, Malhotra et al. demonstrated that miRNAs exemplify tremendous therapeutic potential by functioning as radiosensitive/radioresistance biomarkers for EC in clinical settings [19]. Based on the analysis from the RNA22 and RAID databases, miR-140-5p was predicted as a downstream miRNA of lncRNA CASC15. Existing studies reported that miR-140-5p can inhibit the proliferation, migration, and invasion abilities of gastric cancer; and stimulate chemotherapeutic drug-induced apoptosis in human osteosarcoma [20, 21]. Bioinformatics prediction by RNA22 database in our study further revealed that matrix metalloproteinase 7 (MMP7) might serve as a target gene of miR-140-5p. MMP7 contributes to the progression of cancer invasion and metastasis *via* degradation of the extracellular components [22]. For example, a decreased MMP7 expression can escalate the sensitivity of tumor cells to radiotherapy and

chemotherapy modalities in colon cancer [23]. In recent studies, MMP7 expression has also been associated with EC and linked with advanced tumor-node-metastasis (TNM) stage and invasive grade, indicating the involvement of MMP7 in the progression of EC [24, 25]. With the aforementioned literature serving as basis, MMP7 was considered to be a prognostic marker for ESCC [26].

In the current study, we aimed to analyze the role of the lncRNA CASC15/miR-140-5p/MMP7 axis in ESCC development and the related mechanism. The chief findings suggested the involvement of lncRNA CASC15/miR-140-5p/MMP7 axis in the proliferation, invasion, and apoptosis of ESCC cells, which could further affect the development and radioresistance of ESCC.

RESULTS

lncRNA CASC15 is highly-expressed and associated with a poor prognosis in ESCC

Initially, the expression profiles of lncRNA and mRNA in esophageal mucosa samples obtained from normal individuals and ESCC patients were analyzed using the microarray data. The ESCC-related gene expression dataset GSE45168 in the Gene Expression Omnibus (GEO) database revealed a total of 941 differentially expressed lncRNAs. Amongst them, 5 lncRNAs exhibited significant differences in the expression between the ESCC and normal tissues (Figure 1A), with lncRNA CASC15 being markedly elevated in ESCC tissues (Figure 1B). Meanwhile, the expression profile of lncRNA CASC15 was verified using The Cancer Genome Atlas (TCGA) database, the results of which revealed that the expression of lncRNA CASC15 was evidently augmented in ESCC tissues (Figure 1C), which was consistent with the results obtained from the GEO database. Due to the existence of numerous spliced transcripts in lncRNA CASC15, we designed various forms of primers to detect lncRNA CASC15 expression. The primer #1 exhibiting the highest detection efficiency (Figure 1D), was thus selected for subsequent detection of the lncRNA CASC15 expression patterns. In order to further validate the predicted results, the expression patterns of lncRNA CASC15 in 79 ESCC tissue specimens (including 6 cases in stage I, 31 in stage II, 27 in stage III, and 15 in stage IV) and corresponding adjacent normal tissues were detected using reverse transcription quantitative polymerase chain reaction (RT-qPCR) (Figure 1E), which revealed that lncRNA CASC15 was up-regulated in ESCC tissues, especially in an advanced TNM stage, relative to adjacent normal tissues ($p < 0.05$). Additionally, the

expression of lncRNA CASC15 in the five ESCC cell lines (EC109, TE-1, KYSE70, KYSE270, and KYSE30) and the human esophageal epithelial cell (HEEC) cell line was measured using RT-qPCR. As shown in Figure 1F, compared with the HEEC cell line, all ESCC cell lines exhibited significantly elevated expression profiles of lncRNA CASC15 ($p < 0.05$), with KYSE270 and EC109 cells presenting with the highest lncRNA CASC15 expression. Therefore, the KYSE270 and EC109 cell lines were selected for further experiments. Subsequently, a Kaplan-Meier survival curve was plotted to analyze the correlation between the expression of lncRNA CASC15 and the overall survival rate of ESCC patients (Figure 1G), which revealed a negative correlation between the expression of lncRNA CASC15 and the survival rate of ESCC patients. In addition, as shown in Table 1, the expression of lncRNA CASC15 was irrelevant to parameters such as age, sex and tumor size of ESCC patients, yet being closely associated with the TNM stage, lymph node metastasis (LNM) and differentiation. Conjointly, the

forementioned findings suggested that lncRNA CASC15 was expressed at a higher level in ESCC, and further associated with a poor prognosis of ESCC.

Silencing lncRNA CASC15 inhibits proliferation and invasion of ESCC cells

Since lncRNA CASC15 was extensively expressed in ESCC cells, we chose to silence lncRNA CASC15 using a short hairpin RNA (shRNA) in KYSE270 and EC109 cells to evaluate its effects on ESCC cells. The silencing efficiency was detected by means of RT-qPCR (Figure 2A), which revealed that the expression of lncRNA CASC15 in cells transfected with sh-CASC15 was significantly lower compared to that observed in cells transfected with sh-negative control (NC) ($p < 0.05$), indicating that lncRNA CASC15 was efficiently knocked down. Subsequently, Cell Counting Kit-8 (CCK-8) and Transwell assays were employed to evaluate the viability and invasion of KYSE270 and EC109 cells after lncRNA CASC15 silencing (Figure 2B and 2C). In comparison to the

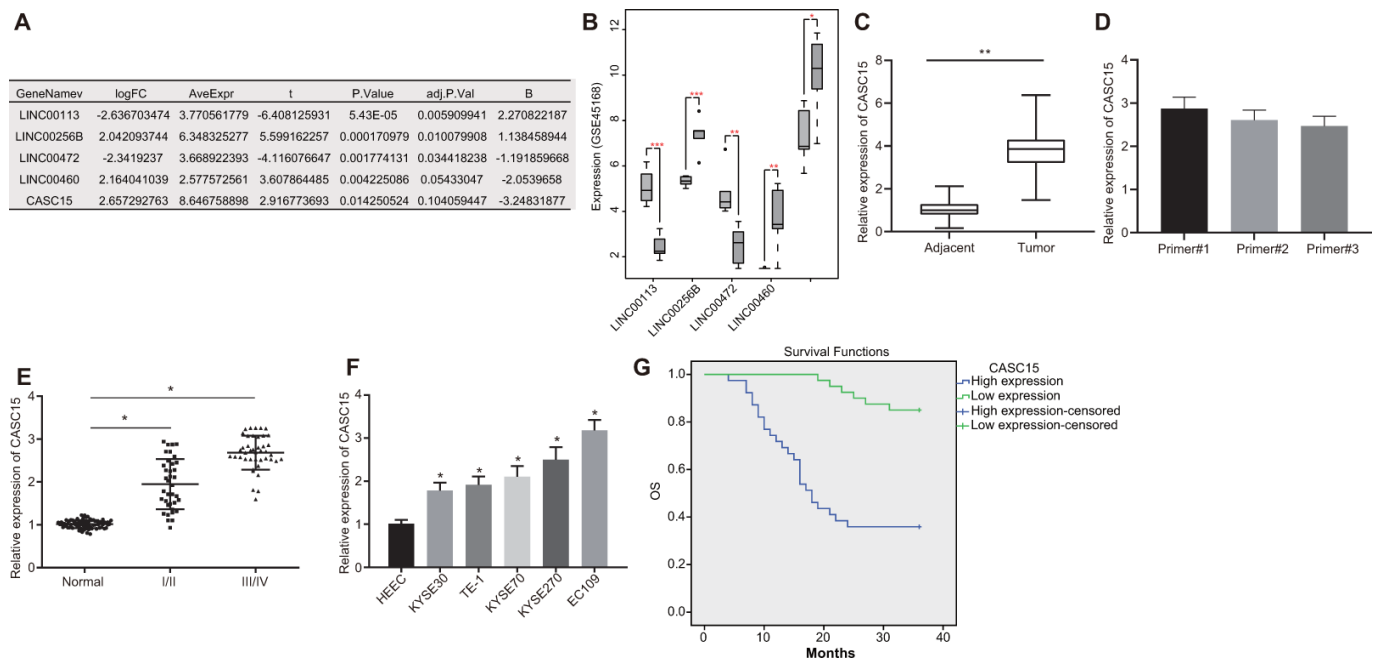


Figure 1. lncRNA CASC15 is overexpressed with poor prognostic value in ESCC. (A) Analysis of five aberrant lncRNAs in ESCC-related gene expression dataset GSE45168 in GEO database. (B) The expression of five aberrant lncRNAs in GSE45168 ($n = 5$). The left box plot represents the expression of lncRNAs in the normal sample, and the right box plot represents the expression of lncRNAs in the ESCC samples). (C) The expression of lncRNA CASC15 in ESCC and adjacent normal tissues analyzed in the TCGA database. (D) The expression of lncRNA CASC15 in EC109 cells detected by different primers. (E) The expression of lncRNA CASC15 in ESCC and adjacent normal tissues ($n = 79$ including 6 cases in stage I, 31 in stage II, 27 in stage III, and 15 in stage IV) determined by RT-qPCR ($*p < 0.05$ vs. the adjacent normal tissues). (F) The expression of lncRNA CASC15 in ESCC cell lines and HEEC cells determined by RT-qPCR ($*p < 0.05$ vs. the HEEC cell line). (G) Kaplan-Meier survival curve to analyze the correlation between lncRNA CASC15 expression and overall survival rate of 79 ESCC patients (log-rank test for the difference significance). The measurement data in panel (D–F) were presented as mean \pm standard deviation and compared with one-way analysis of variance, followed by Tukey's post hoc test.

Table 1. Clinical data of ESCC patients.

Characteristics	Cases	Cases with high CASC15 expression	Percentage	Cases with poor CASC15 expression	Percentage	<i>p</i> value
Age						0.821
> 50 years	34	16	47.06 %	18	52.94 %	
≤ 50 years	45	23	51.11 %	22	48.89 %	
Sex						0.781
Male	64	31	48.44 %	33	51.56 %	
Female	15	8	53.33 %	7	46.67 %	
TNM stage						0.001
I/II stage	53	19	35.85 %	34	64.15 %	
III stage	26	20	76.92 %	6	23.08 %	
Tumor size						0.248
> 3 cm	49	27	55.10 %	22	44.90 %	
≤ 3 cm	30	12	40.00 %	18	60.00 %	
LNM						0.040
Yes	58	33	56.90 %	25	43.10 %	
No	21	6	28.57 %	15	71.43 %	
Differentiation						0.013
High/moderate	44	16	36.36 %	28	63.64 %	
Poor	35	23	65.71 %	12	34.29 %	

Note: ESCC: esophageal squamous cell carcinoma; TNM: tumor node metastasis; LNM: lymph node metastasis.

cells transfected with sh-NC, cells transfected with sh-CASC15 exhibited remarkably decreased viability and invasive abilities ($p < 0.05$). Moreover, Western blot analysis was applied to determine the expression patterns of proliferation-related factor Ki-67 and invasion-related factor MMP2 (Figure 2D and 2E), both of which were evidently reduced upon silencing of lncRNA CASC15 ($p < 0.05$). Thus, these findings suggested that the proliferation and invasion of ESCC cells were decreased after silencing lncRNA CASC15.

lncRNA CASC15 up-regulates MMP7 expression in ESCC by binding to miR-140-5p

Fluorescence *in situ* hybridization (FISH) was performed in order to identify the subcellular localization of lncRNA CASC15 in EC109 cells. As shown in Figure 3A, lncRNA CASC15 was primarily expressed in the cytoplasm of EC109 cells, thereby suggesting the potential function of lncRNA CASC15 as a regulator of EC109 cellular behaviors. Therefore, the downstream miRNAs regulated by lncRNA CASC15 were predicted from the RNA22 database and RAID database, respectively. Moreover, based on the GEO database, we analyzed the ESCC-related

miRNA expression dataset GSE97049 and identified 45 poorly expressed miRNAs in ESCC (Figure 3B). Interestingly, only one intersected miRNA (miR-140-5p) was profound, which was expressed at a low level in ESCC and regulated by lncRNA CASC15 (Figure 3C), signifying the potential regulatory properties of lncRNA CASC15 in ESCC *via* possible regulation of miR-140-5p. As shown in Figure 3D, RT-qPCR further confirmed that the expression of miR-140-5p was down-regulated in both ESCC tissues and cells ($p < 0.05$). Next, we analyzed the correlation between the lncRNA CASC15 and miR-140-5p expression in ESCC tissues (Figure 3E) and cells (Figure 3F). Noticeably, a negative correlation was apparent between the expression of lncRNA CASC15 and miR-140-5p. Additionally, in order to further clarify the downstream regulation mechanism of miR-140-5p, the downstream target genes of miR-140-5p were predicted using the RNA22 database (Figure 3G), and the putative target genes were intersected with the up-regulated genes in GSE45168 dataset. Finally, a sum of 145 potential genes were obtained, which were presented in Figure 3H. Protein-protein interaction correlation analysis exhibited that the MMP7 gene was at the core of these 145 genes (Figure 3I).

Remarkably, a close association between MMP7 and the radiosensitivity of tumors was evident [27, 28]. Thus, it was speculated that the MMP7 gene mediated by miR-140-5p may be involved in the regulation of the radiosensitivity of ESCC. To further ascertain this speculation, the expression patterns of MMP7 and other candidate downstream target genes KCNA2 and S100A14 in ESCC tissues and cells were measured by means of RT-qPCR and Western blot analyses (Figure 3J). The results illustrated that MMP7 was solely up-regulated at mRNA and protein levels in both ESCC tissues and cells ($p < 0.05$), and no significant differences were observed in the expressions of KCNA2 and S100A14 ($p > 0.05$). Thus, MMP7 was chosen as the downstream target of miR-140-5p and lncRNA CASC15 for subsequent research. Next, the effect of miR-140-5p on lncRNA CASC15 and MMP7 was assessed. As displayed in Figure 3K, miR-140-5p could negatively regulate the expression of lncRNA CASC15 and MMP7. The correlation between the

expression of lncRNA CASC15 and MMP7 in ESCC was analyzed, with the results illustrating a positive correlation in Figure 3L. Subsequently, the putative binding sites between lncRNA CASC15 and miR-140-5p, as well as between miR-140-5p and MMP7 were predicted with the help of a biological prediction website (Figure 3M). Dual-luciferase reporter assay was performed to verify the regulatory relationship between lncRNA CASC15 and miR-140-5p as well as the binding relationship between miR-140-5p and MMP7 using recombinant wild type (wt) CASC15/MMP7 and mutant type (mut) CASC15/MMP7 plasmids (Figure 3N–O). In comparison to the EC109 cells transfected with NC mimic, the luciferase signals of wt-CASC15 and wt-MMP7 were noted to be decreased in the EC109 cells transfected with miR-140-5p mimic ($p < 0.05$), but there were no significant differences in the luciferase activities of mut-CASC15 and mut-MMP7 between the EC109 cells transfected with NC mimic and miR-

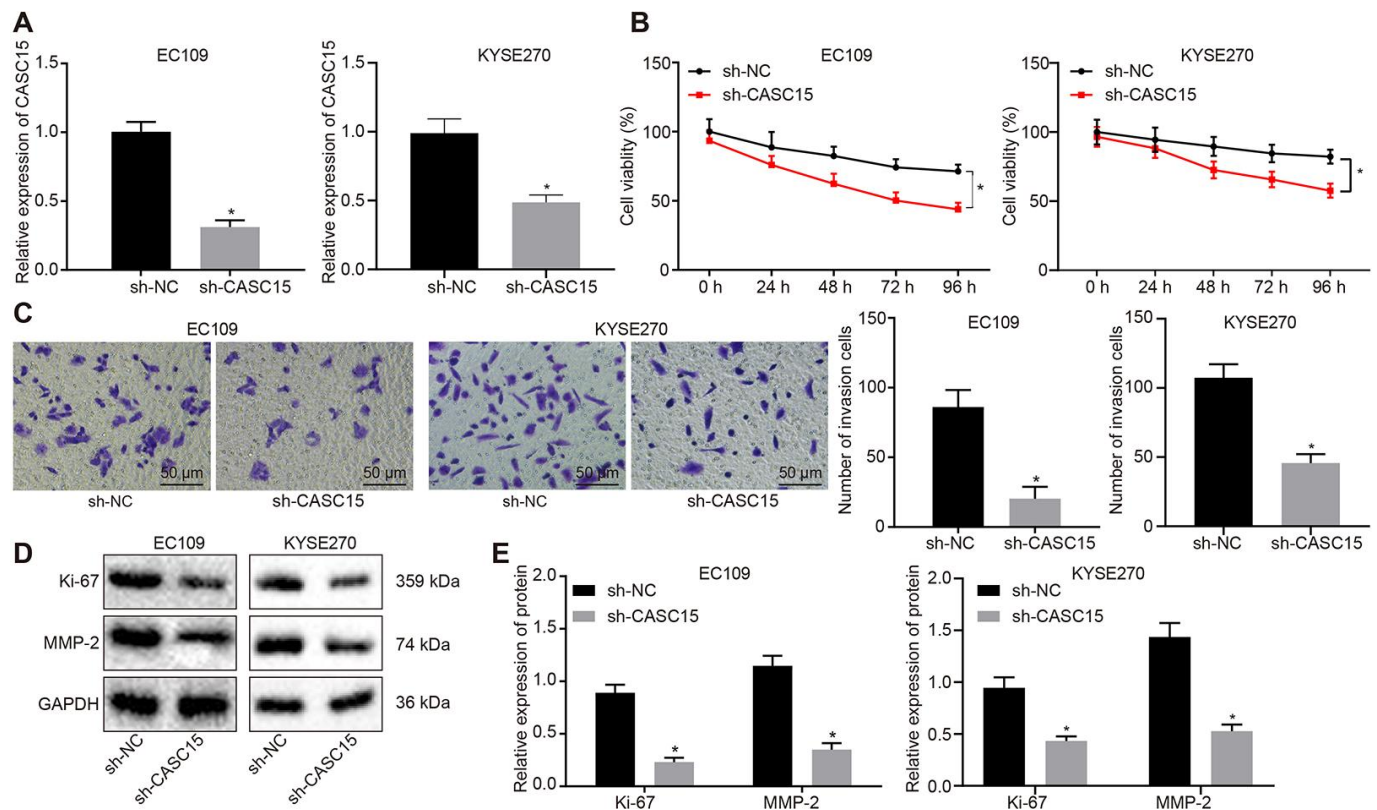


Figure 2. Silencing lncRNA CASC15 reduces the proliferation and invasion of ESCC cells. (A) RT-qPCR to detect the silencing efficiency of lncRNA CASC15. (B) CCK-8 assay to assess the viability of KYSE270 and EC109 cells in response to silencing lncRNA CASC15. (C) Transwell assay to evaluate the invasion of KYSE270 and EC109 cells after silencing lncRNA CASC15 ($\times 200$). (D–E) Western blot analysis to determine the protein level of Ki-67 (a proliferation-related factor) and MMP2 (an invasion-related factor) in KYSE270 and EC109 cells. * $p < 0.05$ vs. the ESCC cells transfected with sh-NC. The measurement data were presented as the mean \pm standard deviation. Data in panel (A, C, E) were analyzed by unpaired t test and those in panel (B) by one-way analysis of variance, followed by Tukey's post hoc test. The experiment was repeated 3 times. sh-NC, cells transfected with negative control plasmids of short hairpin RNA; sh-CASC15, cells transfected with short hairpin RNA against lncRNA CASC15.

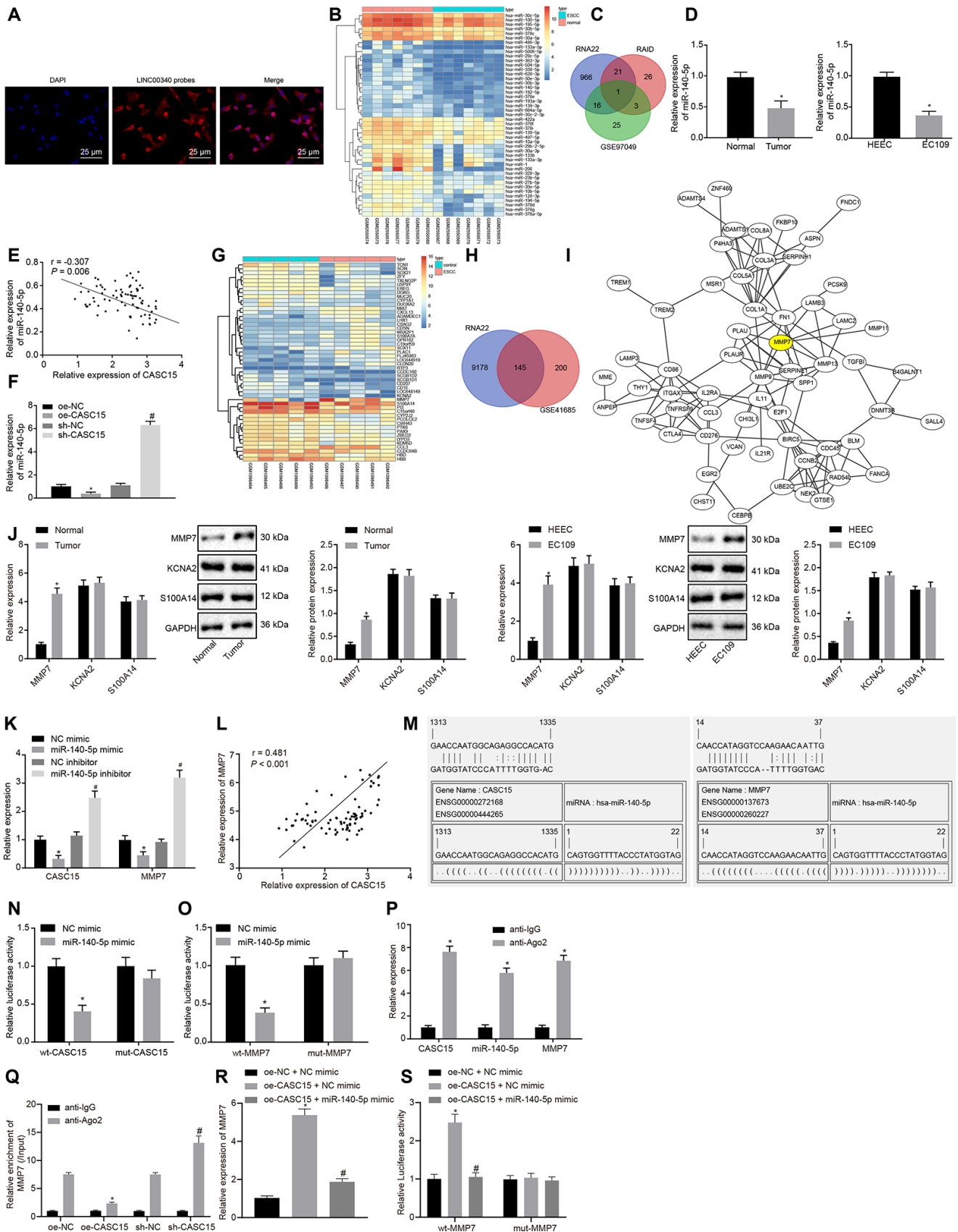


Figure 3. LncRNA CASC15 up-regulates MMP7 expression in ESCC by binding to miR-140-5p. (A) Subcellular localization of lncRNA CASC15 in EC109 cells ($\times 400$). **(B)** A heat map of down-regulated miRNAs in GSE97049 dataset (the X label indicates the

sample number, while the Y label indicates the miRNA name, and each small square indicates the expression of one miRNA in one sample). (C) The intersection of predicted miRNAs regulated by lncRNA CASC15 from RNA 22 database, RAID database and GSE97049 dataset (three circles represent the miRNAs in the RNA 22 database, RAID database and GSE97049 dataset respectively, and the middle part indicates the intersection). (D) RT-qPCR to detect the expression of miR-140-5p in ESCC tissues and cells ($*p < 0.05$ vs. the adjacent normal tissues or HEEC cells). (E) The correlation analysis of lncRNA CASC15 and miR-140-5p expression in ESCC tissues. (F) The correlation between lncRNA CASC15 and miR-140-5p expression in EC109 cells ($*p < 0.05$ vs. EC109 cells transfected with oe-NC, $\#p < 0.05$ vs. EC109 cells transfected with sh-NC). (G) A heat map of differentially expressed genes in GSE45168 dataset (the X axis indicates the sample number, while the Y axis indicates the miRNA name, and each small square indicates the expression of one miRNA in one sample). (H) The intersection of predicted downstream target genes of miR-140-5p from RNA22 database and differentially expressed genes obtained from GSE45168 dataset (two circles indicate up-regulated genes in the predicted results from RNA22 database and GSE45168 dataset, and the middle part indicates their interaction). (I) The correlation analysis of the predicted downstream target genes of miR-140-5p (each circle refers to one gene, and the ligature between two circles represents interaction between two genes). (J) RT-qPCR and Western blot analyses to detect the expression of MMP7 and other candidate target genes (KCNA2 and S100A14) at mRNA and protein levels in ESCC tissues and cells ($*p < 0.05$ vs. the adjacent normal tissues or HEEC cells). (K) RT-qPCR to detect the expression of lncRNA CASC15 and MMP7 measured after upregulating or downregulating miR-140-5p ($*p < 0.05$ vs. EC109 cells transfected with NC mimic, $\#p < 0.05$ vs. EC109 cells treated with NC inhibitor). (L) The correlation analysis between lncRNA CASC15 and MMP7 expression in ESCC. (M) A bioinformatic prediction website to predict the putative binding sites between miR-140-5p and lncRNA CASC15 or MMP7. (N) Dual-luciferase reporter assay to examine the luciferase activity after the co-transfection of miR-140-5p mimic with wt-CASC15 and mut-CASC15. (O) Dual-luciferase reporter assay to test the luciferase activity after the co-transfection of miR-140-5p mimic with wt-MMP7 and mut-MMP7. ($*p < 0.05$ vs. EC109 cells transfected with NC mimic). (P) RIP to assess the enrichment of lncRNA CASC15, miR-140-5p, and MMP7 ($*p < 0.05$ vs. normal mouse IgG). (Q) RIP to study the effect of lncRNA CASC15 on the binding of miR-140-5p and MMP7 ($*p < 0.05$ vs. the treatment of oe-NC anti-Ago2; $\#p < 0.05$ vs. the treatment of sh-NC anti-Ago2). (R) RT-qPCR to detect the mRNA expression of MMP7 in ESCC cells ($*p < 0.05$ vs. the treatment of oe-NC and NC mimic; $\#p < 0.05$ vs. the treatment of oe-CASC15 and NC mimic). (S) Dual-luciferase reporter assay to test the luciferase activity after the co-transfection of oe-CASC15 + miR-140-5p mimic with wt-MMP7 and mut-MMP7 ($*p < 0.05$ vs. EC109 cells transfected with oe-NC + NC mimic; $\#p < 0.05$ vs. EC109 cells transfected with oe-CASC15 + NC mimic). The measurement data were presented as the mean \pm standard deviation. Data in panel (D) (left) and (J) (left) were analyzed by paired *t* test and those in panel (D) (right) and (F, J) (right) and (K, N, O, P, Q, R, S) by unpaired *t* test; the experiment was repeated 3 times. NC mimic, EC109 cells transfected with negative control plasmids of mimic; miR-140-5p mimic, EC109 cells transfected with miR-140-5p mimic; oe-NC, EC109 cells transfected with negative control plasmids of overexpression vector; sh-NC, EC109 cells transfected with negative control plasmids of short hairpin RNA; wt-CASC15, EC109 cells transfected with luciferase reporter plasmids containing wild-type lncRNA CASC15; mut-CASC15, EC109 cells transfected with luciferase reporter plasmids containing mutant lncRNA CASC15; wt-MMP7, EC109 cells transfected with luciferase reporter plasmids containing wild-type MMP7; mut-MMP7, EC109 cells transfected with luciferase reporter plasmids containing mutant MMP7.

140-5p mimic ($p > 0.05$). The binding relationship between lncRNA CASC15 and miR-140-5p or between lncRNA CASC15 and MMP7 was detected using the RNA-binding protein immunoprecipitation (RIP) experiment (Figure 3P). In comparison to the anti-IgG control, cells treated with anti-Ago2 exhibited significantly increased enrichment of miR-140-5p, lncRNA CASC15, and MMP7 ($p < 0.05$). Thereafter, to further verify the aforementioned finding, RIP was performed to assess the amount of MMP7 mRNA interacting with miR-140-5p in response to over-expression or knockdown of CASC15. The results revealed that the amount of MMP7 mRNA interacting with miR-140-5p was reduced after lncRNA CASC15 over-expression, yet opposite trends were noted upon lncRNA CASC15 silencing ($p < 0.05$) (Figure 3Q). Moreover, RT-qPCR (Figure 3R) and dual-luciferase reporter assay (Figure 3S) revealed that mRNA expression and luciferase activity of MMP7 were elevated after lncRNA CASC15 over-expression, which was rescued by miR-140-5p elevation ($p < 0.05$). With these results as basis, we speculated that lncRNA CASC15 may bind

to miR-140-5p in ESCC, thereby up-regulating the expression of MMP7.

lncRNA CASC15 inhibits the radiosensitivity of ESCC by down-regulating miR140-5p and up-regulating MMP7

In order to investigate the regulatory role of lncRNA CASC15 in response of radiosensitivity against ESCC, the expression patterns of lncRNA CASC15, miR-140-5p, and MMP7 in the radiotherapy-sensitive and radiotherapy-resistant ESCC patients were determined by means of RT-qPCR (Figure 4A) and Western blot analyses (Figure 4B). Results unraveled that the expressions of lncRNA CASC15 and mRNA and protein expression of MMP7 were higher, while those of miR-140-5p were lower in radiotherapy-resistant patients compared to radiotherapy-sensitive patients ($p < 0.05$). Meanwhile, the expression of lncRNA CASC15 was further determined in the ESCC parental cell line TE-1 and radiation-resistant cell line TE-1R (Figure 4C). It was found that lncRNA CASC15 was expressed at a high level in the TE-1R cell line relative to the TE-1 line ($p <$

0.05). The aforementioned findings suggested that the lncRNA CASC15/miR-140-5p/MMP7 axis affected the radiosensitivity against ESCC.

Furthermore, to investigate the role of this axis in the radiosensitivity of ESCC cells, KYSE270 and EC109 cells were transfected with different plasmids (including NC mimic, miR-140-5p mimic, sh-NC, sh-MMP7, sh-CASC15, oe-NC, oe-CASC15) and irradiated with 4 Gy X-ray. The transfection efficiency was detected by means of RT-qPCR (Figures 4D and 5A), which

demonstrated that the transfection efficiency reached the required threshold for further experiments. Next, cell viability was measured by conducting a CCK-8 assay (Figure 4E and 5B). The results revealed that compared to the matched controls, over-expression of lncRNA CASC15 in KYSE270 and EC109 cells at 4 Gy significantly enhanced cell viability ($p < 0.05$), which was reversed by knocking down MMP7 ($p < 0.05$). Besides, decreased cell viability was evident following the treatment of single miR-140-5p mimic or sh-MMP7 at 4 Gy ($p < 0.05$). Cell apoptosis was then determined

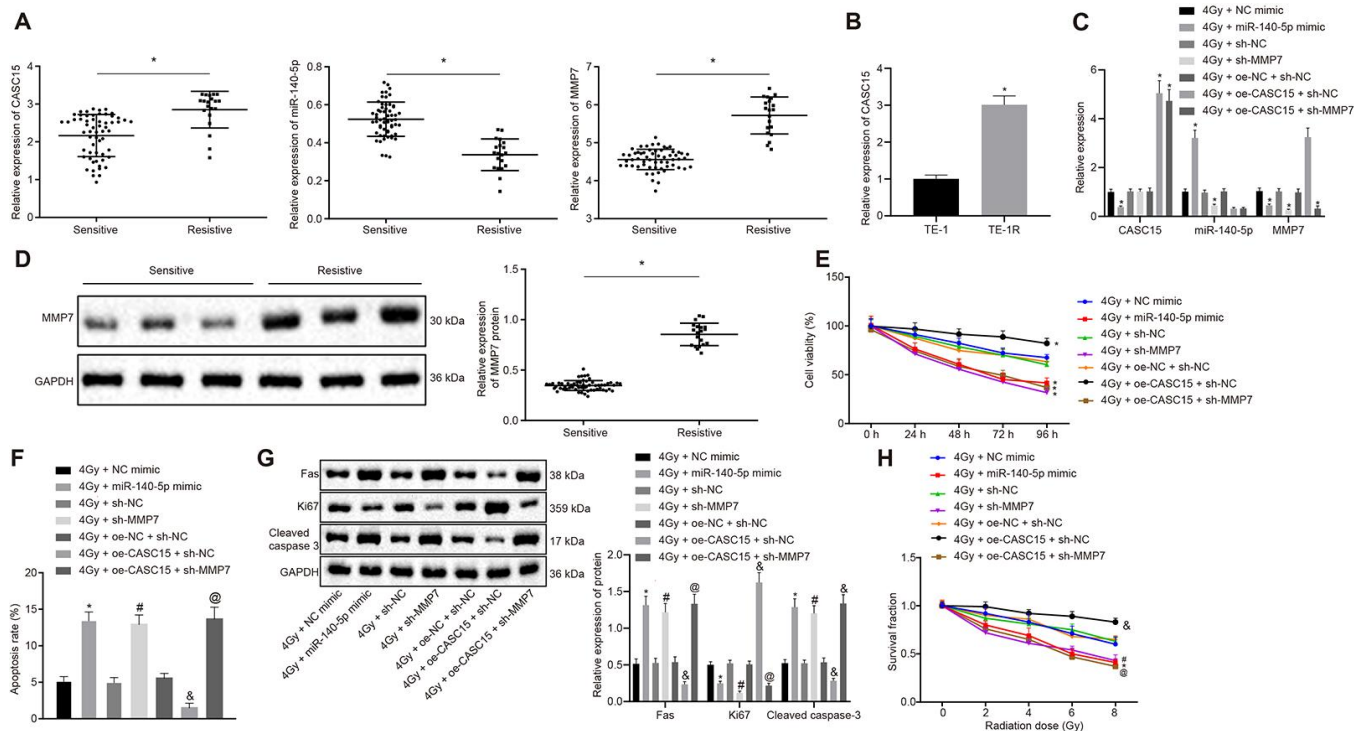


Figure 4. LncRNA CASC15 inhibits the sensitivity of ESCC to radiotherapy by decreasing miR-140-5p and upregulating MMP7.

(A) RT-qPCR to detect the expression of lncRNA CASC15, miR-140-5p, and MMP7 in the radio-sensitive and radio-resistant ESCC patients ($*p < 0.05$ vs. the sensitive group). (B) Western blot analysis to measure the protein expression of MMP7 in the radio-sensitive and radio-resistant ESCC patients ($*p < 0.05$ vs. the sensitive group). (C) RT-qPCR to determine the expression of lncRNA CASC15 in ESCC naive cell line TE-1 and radiation resistant cell line TE-1R ($*p < 0.05$ vs. ESCC parental cell line TE-1). (D) RT-qPCR to test the transfection efficiency in EC109 cells. (E) CCK-8 assay to evaluate cell viability of EC109 cells. (F) Flow cytometry to assess cell apoptosis of EC109 cells. (G) Western blot analysis to determine the protein level of Fas, Ki-67 and cleaved Caspase 3 in EC109 cells. (H) Clone formation ability of EC109 cells after X-ray radiation. In panel (C–G), $*p < 0.05$ vs. EC109 cells transfected with 4 Gy + NC mimic. $\#p < 0.05$ vs. EC109 cells transfected with 4 Gy + sh-NC. $\&p < 0.05$ vs. EC109 cells transfected with 4 Gy + oe-NC + sh-NC; $@p < 0.05$ vs. EC109 cells transfected with 4 Gy + oe-CASC15 + sh-NC. The measurement data were presented as the mean \pm standard deviation. Data in panel (A, B) were analyzed by unpaired t test, and data in panel (C, E, F) were analyzed by one-way analysis of variance, followed by Tukey's post hoc test. Data in panel D were analyzed by repeated-measures analysis of variance, followed by Tukey's post hoc test, and data in panel (E) were analyzed by two-way analysis of variance, followed by Tukey's post hoc test; the experiment was repeated 3 times. 4 Gy + NC mimic, EC109 cells transfected with negative control of mimic and treated with 4 Gy irradiation; 4 Gy + miR-140-5p mimic, EC109 cells transfected with miR-140-5p mimic and treated with 4 Gy irradiation; 4 Gy + sh-NC, EC109 cells transfected with negative control plasmids of short hairpin RNA and treated with 4 Gy irradiation; 4 Gy + sh-MMP7, EC109 cells transfected with short hairpin RNA against matrix metalloproteinase 7 and treated with 4 Gy irradiation; 4 Gy + oe-NC + sh-NC, EC109 cells transfected with negative control plasmids of overexpression vector and short hairpin RNA and treated with 4 Gy irradiation; 4 Gy + oe-CASC15 + sh-NC, EC109 cells transfected with plasmids overexpressing lncRNA CASC15 and negative control of short hairpin RNA and treated with 4 Gy irradiation; 4 Gy + oe-CASC15 + sh-MMP7, EC109 cells transfected with plasmids overexpressing lncRNA CASC15 and short hairpin RNA against matrix metalloproteinase 7 and treated with 4 Gy irradiation.

by conducting flow cytometry (Figure 4F and 5C), the results of which suggested that over-expression of lncRNA CASC15 in KYSE270 and EC109 cells irradiated with 4 Gy remarkably decreased cell apoptosis ($p < 0.05$), which could be overturned by silencing MMP7 ($p < 0.05$). The treatment of single miR-140-5p mimic or sh-MMP7 at 4 Gy exclusively induced apoptosis ($p < 0.05$). Western blot analysis was conducted to determine the expression patterns of

proliferation-related factor Fas and Ki-67 and apoptosis-related factor cleaved Caspase 3. As shown in Figure 4G and 5D, KYSE270 and EC109 cells transfected with oe-CASC15 at 4 Gy showed increased expression of Ki-67 and dropped expression of Fas and cleaved caspase-3, while co-transfection of sh-MMP7 inhibited the effects of oe-CASC15 on Fas, Ki-67 and cleaved Caspase-3 levels ($p < 0.05$). In addition, a single transfection of the miR-140-5p mimic or sh-MMP7

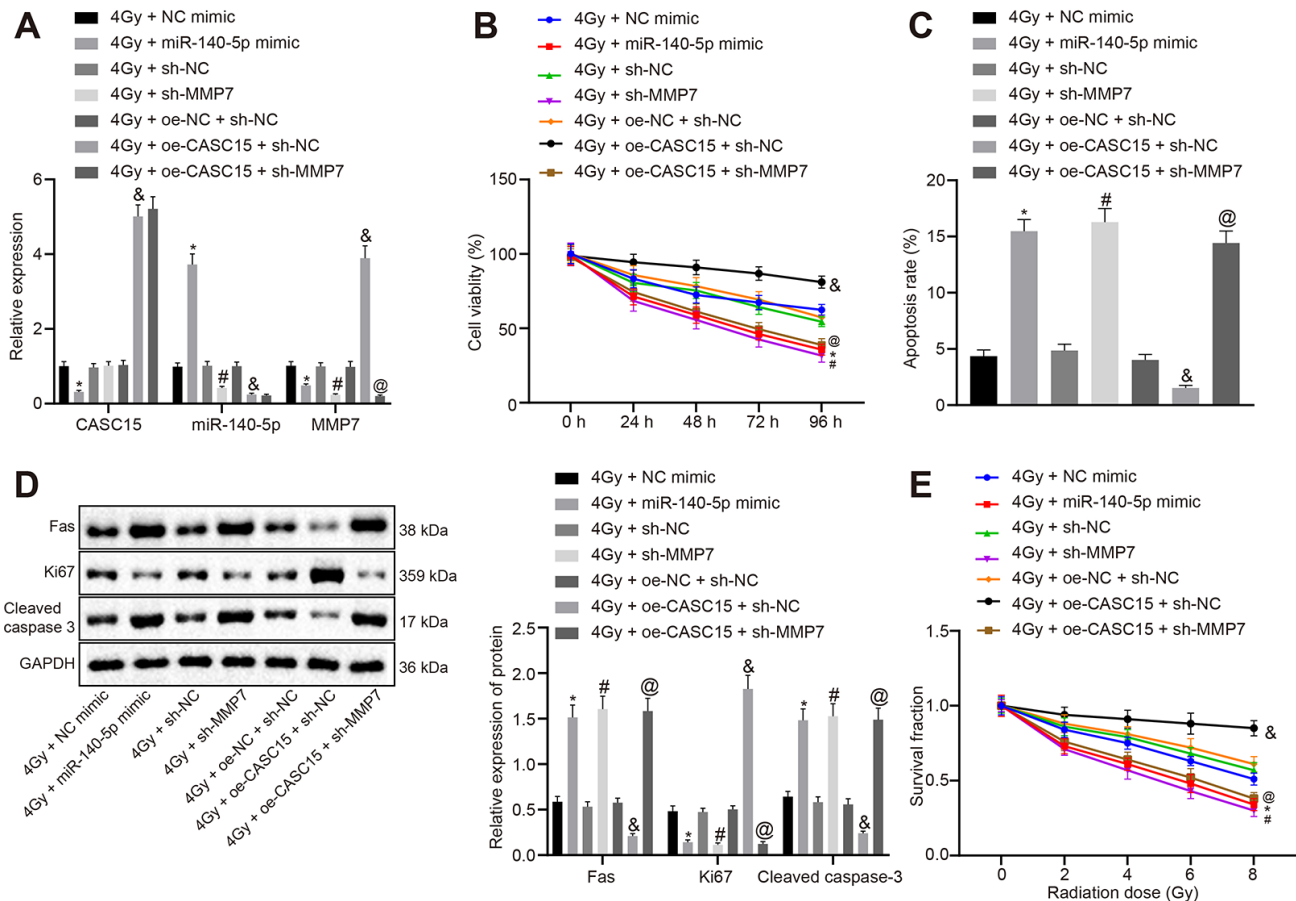


Figure 5. LncRNA CASC15 impairs the radiosensitivity of ESCC by decreasing miR-140-5p and elevating MMP7. (A) RT-qPCR to test the transfection efficiency in KYSE270 cells. (B) CCK-8 assay to assess cell viability of KYSE270 cells. (C) Flow cytometry to evaluate cell apoptosis of KYSE270 cells. (D) Western blot analysis to determine the protein level of Fas, Ki-67 and cleaved Caspase 3 in KYSE270 cells. E, Clone formation ability of KYSE270 cells after X-ray radiation. * $p < 0.05$ vs. KYSE270 cells transfected with 4 Gy + NC mimic; # $p < 0.05$ vs. KYSE270 cells transfected with 4 Gy + sh-NC; & $p < 0.05$ vs. KYSE270 cells transfected with 4 Gy + oe-NC + sh-NC; @ $p < 0.05$ vs. KYSE270 cells transfected with 4 Gy + oe-CASC15 + sh-NC. The measurement data were presented as the mean \pm standard deviation. Data in panel (A, C, D) were analyzed by one-way analysis of variance, followed by Tukey's post hoc test. Data in panel B were analyzed by repeated-measures analysis of variance, followed by Tukey's post hoc test, and data in panel C were analyzed by two-way analysis of variance, followed by Tukey's post hoc test; the experiment was repeated 3 times. 4 Gy + NC mimic, KYSE270 cells transfected with negative control of mimic and treated with 4 Gy irradiation; 4 Gy + miR-140-5p mimic, KYSE270 cells transfected with miR-140-5p mimic and treated with 4 Gy irradiation; 4 Gy + sh-NC, KYSE270 cells transfected with negative control plasmids of short hairpin RNA and treated with 4 Gy irradiation; 4 Gy + sh-MMP7, KYSE270 cells transfected with short hairpin RNA against matrix metalloproteinase 7 and treated with 4 Gy irradiation; 4 Gy + oe-NC + sh-NC, KYSE270 cells transfected with negative control plasmids of overexpression vector and short hairpin RNA and treated with 4 Gy irradiation; 4 Gy + oe-CASC15 + sh-NC, KYSE270 cells transfected with plasmids overexpressing lncRNA CASC15 and negative control of short hairpin RNA and treated with 4 Gy irradiation; 4 Gy + oe-CASC15 + sh-MMP7, KYSE270 cells transfected with plasmids overexpressing lncRNA CASC15 and short hairpin RNA against matrix metalloproteinase 7 and treated with 4 Gy irradiation.

weakened the expression patterns of Ki-67 and augmented the expression profiles of Fas and cleaved Caspase-3. Moreover, KYSE270 and EC109 cells were treated with 0, 2, 4, 6, and 8 Gy X-ray respectively, and then clone formation experiments were conducted (Figure 4H and 5E). Results demonstrated that lncRNA CASC15 could potentially enhance the clone forming ability of KYSE270 and ESCC cells at variable doses of X-ray ($p < 0.05$), which was prevented after down-regulation of MMP7 ($p < 0.05$). Moreover, the clone forming ability was also diminished after miR-140-5p elevation and MMP7 inhibition ($p < 0.05$). Thus, the aforementioned results indicated that lncRNA CASC15 inhibited the sensitivity of ESCC to radiotherapy by down-regulating miR-140-5p and up-regulating MMP7.

Silencing lncRNA CASC15 increases the radiosensitivity of ESCC *in vivo*

In an attempt to assess the effect of lncRNA CASC15 on the radiosensitivity of ESCC *in vivo*, nude mice were injected with KYSE270 and EC109 cells infected with a lentivirus containing sh-CASC15. Upon observing the mean volume of tumors approaching 300 mm³, the mice were irradiated once a week by 4 Gy X-ray. The volume of tumors was measured every 3 days after irradiation, and the nude mice were euthanized 21 days later with the tumors collected. As detected by RT-qPCR, the lncRNA CASC15 was efficiently impeded by lentivirus-packaged shRNA, after which the expression of miR-140-5p was increased while that of MMP7 was reduced in tumors (Figure 6A) ($p < 0.05$). Moreover, the volume and weight of tumors were found to be lower after treatment with 4 Gy and sh-CASC15 relative to treatment with 4 Gy and sh-NC (Figure 6B and 3C) ($p < 0.05$). Then, the expression patterns of Ki-67 and cleaved Caspase 3 and MMP7 in tumors were measured by means of Western blot and immunohistochemistry (IHC) analyses (Figure 6D and 6E), which revealed that treatment with 4 Gy and sh-CASC15 led to a reduction in the level of Ki-67, and an elevation in the level of cleaved Caspase 3 and MMP7 in contrast to the treatment with 4 Gy and sh-NC ($p < 0.05$). These results demonstrated that silencing lncRNA CASC15 could effectively increase the radiosensitivity of ESCC *in vivo*.

DISCUSSION

ESCC affects millions of individuals across the world, accompanied by alarmingly high mortality rates. ESCC patients are often diagnosed at late stage due to frequent local/distant metastasis and poor subjective symptoms [29]. Unfortunately, radioresistance is a common challenge faced during treatment which decreases the efficiency of ESCC radiotherapy [10]. Thus, elucidation of the underlying regulatory mechanisms of radiosensitivity and

the key molecules capable of enhancing the sensitivity of ESCC treatments could be highly rewarding in regard to improving the outcomes of patients plagued by ESCC. In the current study, we ascertained the hypothesis supporting that down-regulating lncRNA CASC15 may enhance the radiosensitivity of ESCC *via* miR-140-5p-mediated inhibition of MMP7.

Initially, our findings revealed that lncRNA CASC15 was over-expressed in ESCC, which was associated with ESCC radiosensitivity. Specifically, over-expression of lncRNA CASC15 enhanced ESCC cell viability while decreasing cell apoptosis. Lessard et al. documented robust levels of lncRNA CASC15 during melanoma progression, whereas silencing lncRNA CASC15 decreased the proliferation and invasion abilities of melanoma cells [30]. Another study demonstrated that lncRNA CASC15 was up-regulated in pediatric B-acute lymphoblastic leukemia, which highlighted the ability of an enforced lncRNA CASC15 expression to reduce colony formation and engraftment [31]. Similarly, lncRNA CASC15 has been observed to be specifically up-regulated in tongue squamous cell carcinoma (TSCC), and its down-regulation was further found to comprehensively impede the proliferation, cell cycle, and migration of TSCC cells [32]. Meanwhile, Shen et al. also indicated the association of various other lncRNAs with the prognosis and chemoradiotherapy resistance in ESCC, including LOC285194, urothelial carcinoma-associated 1 (UCA1), and metastasis-associated lung adenocarcinoma transcript 1 (MALAT-1) [33].

Additionally, the current study uncovered the interaction among lncRNA CASC15, miR-140-5p, and MMP7, due to their involvement in the regulation of radiosensitivity to ESCC. Our experiments verified the ability of lncRNA CASC15 to competitively bind to miR-140-5p in accordance with the finding of the RNA22 database. Furthermore, our evidence further proved that lncRNA CASC15 could play a suppressive role in the radiosensitivity of ESCC *via* its ability to down-regulate miR-140-5p. Moreover, existing studies have demonstrated that over-expression of lncRNA AK022798 enhances cisplatin-resistant gastric cancer formation, due to the function of lncRNA HOX antisense intergenic RNA to function as a competitive endogenous RNA to foster cisplatin resistance in gastric cancer [34, 35]. Several studies have also indicated the tumor suppressor or promoter role of miRNAs owing to their ability to function in the progression of the tumorigenic processes of various malignant tumors including ESCC [36, 37]. What's more, the vitality of miRNAs due to their extensive function has been well-documented in the development and susceptibility of ESCC. For instance, enhancement of miR-142-3p

expression is coherent with poor prognosis of ESCC patients and has been established as an independent prognostic factor in ESCC [38]. Moreover, miR-143 was associated with the recurrence and invasion depth of ESCC and epigenetic activation of miR-143 owing to

the contribution of radiosensitizer curcumin towards enhancing the radiosensitivity of prostate cancer and further inhibiting growth and inducing apoptosis of cancer cells respectively [39, 40]. Down-regulation of miR-140-5p by lncRNA SNHG16 can also bring about

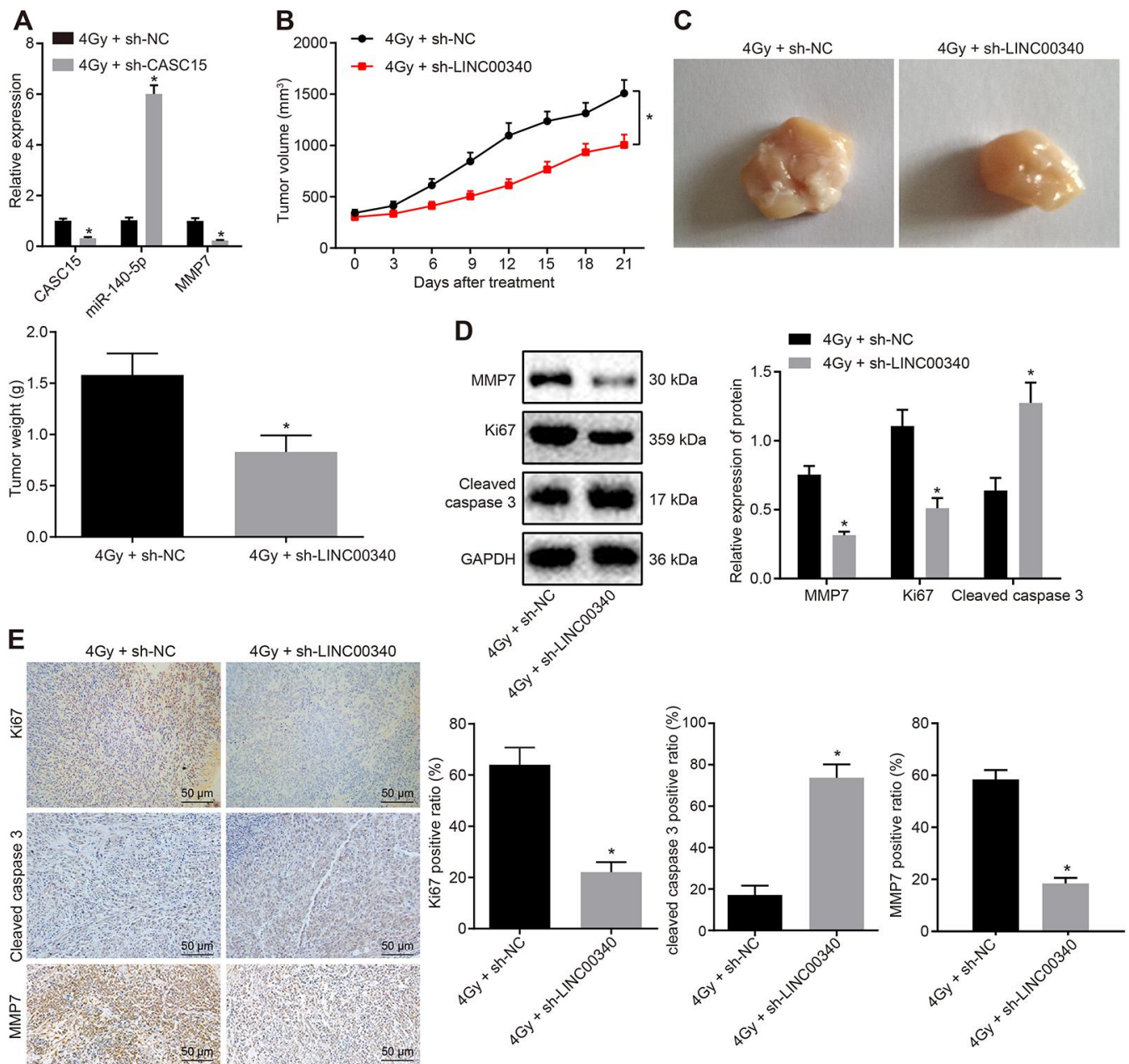


Figure 6. Silencing lncRNA CASC15 increases the radiosensitivity of ESCC *in vivo*. (A) RT-qPCR to detect the silencing efficiency of lncRNA CASC15 and the expression of miR-140-5p and MMP7 in tumors. (B) The volume of tumors following X-ray radiation and lncRNA CASC15 silencing. (C) The weight of tumors following X-ray radiation and lncRNA CASC15 silencing. (D) The levels of MMP7, Ki-67 and cleaved Caspase 3 in tumors in response to X-ray radiation and lncRNA CASC15 silencing determined by Western blot analysis. (E) The levels of MMP7, Ki-67 and cleaved Caspase 3 in tumors in response to X-ray radiation and lncRNA CASC15 silencing detected by IHC analysis ($\times 200$). * $p < 0.05$ vs. the 4 Gy + sh-NC group. $n = 12$. The measurement data were presented as the mean \pm standard deviation. Data in panel (A, C–E) were analyzed by unpaired *t* test and panel B by repeated-measures analysis of variance, followed by Tukey's post hoc test; the experiment was repeated 3 times. 4 Gy + sh-CASC15, 4 Gy irradiated mice with EC109 cells infected with lentivirus containing shRNA targeting CASC15, 4 Gy + sh-NC, 4 Gy irradiated mice with EC109 cells infected with lentivirus containing negative control shRNA.

increases in EC cell proliferation, migration, and epithelial-to-mesenchymal transition [41]. Remarkably, our investigation illustrated that MMP7 was indeed a target gene of miR-140-5p. As a marker associated with tumor cell migration and invasion, MMP7 up-regulation has been correlated with advanced tumor stage and LNM in EC [24]. A recent research further evidenced the promotive effect of MMP7 on TSCC cell migration and invasion abilities [42]. MMP7 expression is also extensively associated with variations in chemoresistance, and known to function as a prognostic factor in several solid tumors, including non-small cell lung cancer and colorectal cancer [43, 44]. MMP7 was associated with the acquisition of colon cancer chemoresistance *via* Fas/FasL system [45]. Furthermore, an existing study verified the ability of cancer cells to induce apoptosis resistance through up-regulation of MMP7 [46]. In addition to chemoresistance, MMP7 has been previously illustrated to exhibit an association with the outcome of preoperative chemoradiotherapy in rectal cancer [47], and its knockdown could impede the proliferative property of colon cancer cells and enhance the radiosensitivity [23]. Our results further demonstrated the significance of MMP7 as a potential modulator to impede the radiosensitivity of ESCC. Several miRNAs can impact cancer progression and metastasis through direct and indirect mechanisms with MMPs [48]. For instance, miR-34a inhibited the

cell migration and invasion upon interacting with MMP2 and MMP9 in ESCC [49]. In addition, Osako et al. substantiated the pivotal role of the miR-375/MMP13 axis against ESCC aggressiveness [50]. Meanwhile, Wu et al. indicated that miR-140 targeting MMP13 could comprehensively suppress prostate cancer cell migration and invasion [51]. Activation of MMP7 also contributes to preventing cisplatin-induced apoptosis, consequently enhancing chemoresistance of lung cancer [52]. The potential mechanism for the accelerative role CASC15 played in the proliferation and radiosensitivity of ESCC cells may be attributed to the inhibition of miR-140-5p, or the enhancement of MMP7, which is associated with the DNA damage/repair pathway. In conclusion, lncRNA CASC15 could enhance the radiosensitivity of ESCC by impeding the cell proliferate ability and apoptosis resistance *via* blocking miR-140-5p-dependent down-regulation of MMP7.

Furthermore, we found that the decreased MMP7 expression could reverse the Ki-67 over-expression and cleaved Caspase 3 deficiency elicited by up-regulated expression of lncRNA CASC15. Caspase 3 is the primary executioner caspase in the process of apoptosis and detrimental to the process itself [53]. Ki-67, a clinical marker employed for proliferating cells, is a nuclear protein possessing the specific cell-cycle dependent

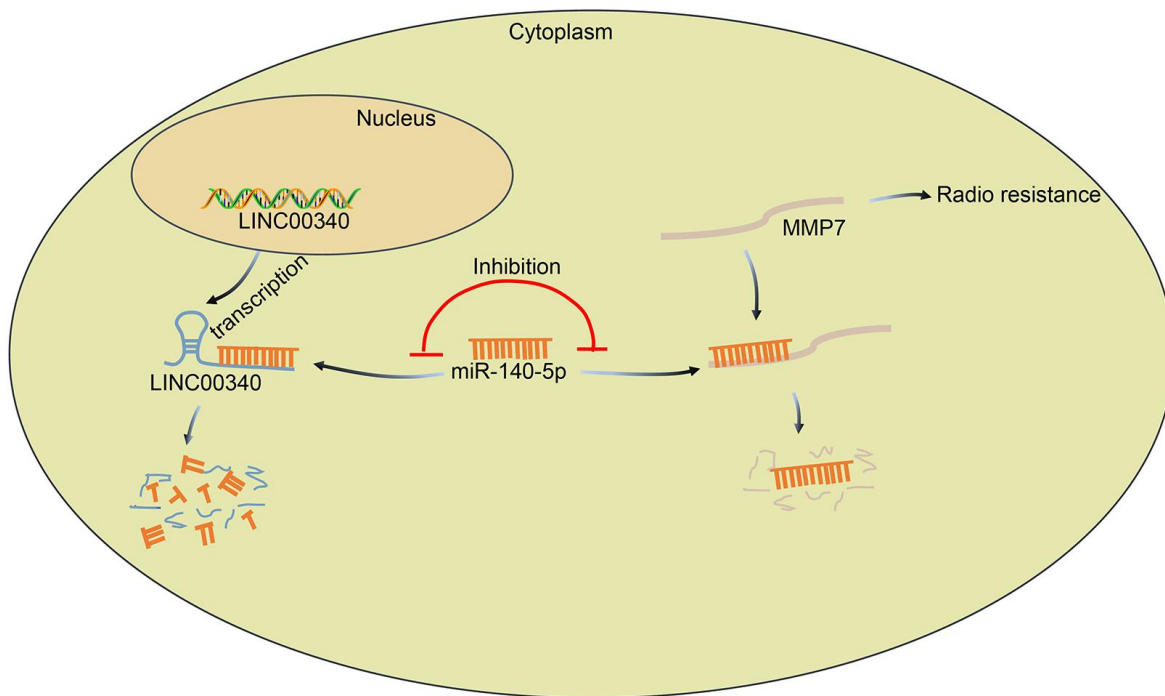


Figure 7. The regulatory mechanism of lncRNA CASC15/miR-140-5p/MMP7 axis involving in radiosensitivity of ESCC. lncRNA CASC15 up-regulates MMP7 expression in ESCC by binding to miR-140-5p, which promotes the proliferation and invasion of ESCC cells and further reduces the radiosensitivity of ESCC.

expression profile [54]. Ki-67 has also been established as a potential prognostic factor for breast cancer patients undergoing postmastectomy radiotherapy, while cleaved Caspase 3 can function as comprehensive biomarkers for tumorigenesis in patients diagnosed with oral TSCC [55, 56]. Decreased lncRNA CASC15 expressions have also been known to result in elevated expression profiles of several apoptosis-related proteins (Bax, cleaved Caspase-3, and PARP) in hepatocellular carcinoma and may facilitate the proliferation by inhibiting the intrinsic apoptosis pathway [17].

To conclude, the key findings from our study suggest that silencing lncRNA CASC15 enhances the radiosensitivity of ESCC through miR-140-5p-dependent inhibition of MMP7 (Figure 7). Our research provides an insight on a set of novel targets among the 145 potential target genes of miR-140-5p linked to regulation of radiosensitivity. However, due to the limitation of time and expenditure, this research has not been further excavated at present, which proposes the need for future studies to extrapolate the complete therapeutic effects of the lncRNA CASC15/miR-140-5p/MMP7 axis. Besides, the identification of lncRNA CASC15/miR-140-5p/MMP7 axis in radiosensitivity of ESCC may facilitate the understanding of the resistance of ESCC to chemotherapy.

MATERIALS AND METHODS

Ethical statement

The current study protocols were approved by the Ethics Committee of Affiliated Cancer Hospital of Zhengzhou University (Henan Cancer Hospital). Signed informed consents were obtained from all participants prior to enrollment. All animal experiments were in accordance with the guidelines issued in the Guide for the Care and Use of Laboratory Animal by National Institutes of Health, and great efforts were made to minimize the suffering of the included animals.

Bioinformatics prediction

Microarray data, including data related to cancerous and normal tissues from ESCC patients, were retrieved from the GEO database (<https://www.ncbi.nlm.nih.gov/geo/>). Subsequently, the differentially expressed lncRNAs were identified using the Limma package of R language, with the cut-off value set at $p < 0.05$ and $|\log_2(\text{fold change})| > 2$. The most significant differentially expressed lncRNAs in ESCC-related microarray were verified in the TCGA. After the lncRNAs were screened, their downstream miRNAs were predicted using the RNA22 (<https://cm.jefferson.edu/rna22/Precomputed/OptionController?species=HomoSapiens>) and RAID database (<http://www.rna-society.org/raid/>

[search.html](#)). Moreover, the target genes of the candidate miRNA were further predicted using the RNA22 database (<https://cm.jefferson.edu/rna22/Precomputed/>). Subsequently, the protein interaction network was obtained from the String database (<https://string-db.org/>).

Study subjects

ESCC tissues and adjacent normal tissues were obtained from ESCC patients who underwent esophagectomy at the Affiliated Cancer Hospital of Zhengzhou University (Henan Cancer Hospital) between February 2016 and July 2017, which were preserved in liquid nitrogen. None of the included patients underwent chemotherapy or radiotherapy or any other comprehensive anti-tumor therapies prior to tissue collection. Patients were staged according to the criteria of the American Joint Commission for Cancer (AJCC).

Furthermore, 79 additional patients clinically diagnosed with ESCC at the Affiliated Cancer Hospital of Zhengzhou University (Henan Cancer Hospital) between April 2016 and June 2018 were selected and assigned into the sensitive group and the resistant group after instilling a two-month regimen of radiotherapy. The clinical criteria employed to categorize patients into the sensitive group and the resistant group were as follows: the position of the patients was fixed by the body membrane or neck and shoulder membrane, and breast computed tomography (CT) was applied to enhance the scan orientation with series scanning through 5 mm of thickness. In addition, a three-dimensional treatment planning system was transmitted through the network system. The target region, which was defined based on the 50th and 62nd reporting principles of the International Commission Radiological Units (ICRU), was plotted in reference to the breast CT and esophagus barium meal X ray images. Then, the target regions of the primary tumor (GTV-T) and metastatic lymph nodes (GTV-N), clinical target volume (CTV, GTV-T's external expansion of 0.6 - 0.8 cm at horizontal level; manually modified after external expansion of 3 - 5 cm toward head or foot), planning target volume (PTV, CTV's external expansion of 0.5 cm) and organ at risk were plotted. Next, 6 MV-X ray was employed for conducting three-dimensional conformal radiation therapy (3DCRT) or intensity modulated radiation therapy (IMRT) (1.8 - 2.2 Gy/time; 5 times/week; total dose, 57 - 67 Gy; median dose, 60.2 Gy). Four weeks after being subjected to the radiotherapy, esophageal barium meal examination was conducted. Patients with complete or partial remission were regarded as the sensitive group, and those with non-remission as the resistant group. Those patients comprised of 64 males and 15 females, with a

calculated mean age of (50.44 ± 9.15) years. No significant differences were evident in terms of age and sex between the sensitive and resistant groups. The enrolled ESCC patients were identified with the following clinical manifestations: 1) not underwent radiotherapy before surgery; 2) normal functions of other organs such as the heart, lung, liver, and kidney; 3) no distant metastasis or other malignant tumors. Relevant clinical data are shown in Table 1.

Cell treatment

Normal HEEC cell line along with five ESCC cell lines (EC109, TE-1, KYSE70, KYSE270, and KYSE30) were purchased from the American Type Culture Collection (ATCC, Manassas, VA, USA). The cells were cultured in high glucose Dulbecco's modified eagle's medium (DMEM) supplemented with 10% fetal bovine serum (FBS, Gibco, Carlsbad, CA, USA) at 37°C under saturated humidity containing 95% air and 5% CO₂, which were subcultured upon reaching 90% confluence. RT-qPCR was then conducted to screen the cell line with the highest expression of lncRNA CASC15, among which the KYSE270 and EC109 cell lines exhibiting the highest expression of lncRNA CASC15 were chosen for the follow-up experiments. The TE-1R cell line resistant to radiation was screened following the principles of a former study [57, 58].

Then, the cells were plated in 6-well plates and transfected with the following plasmids using lipofectamine 2000 (Invitrogen, Carlsbad, CA, USA) according to the provided instructions, including shRNA against lncRNA CASC15 (sh-CASC15), miR-140-5p mimic, shRNA against MMP7 (sh-MMP7), plasmid over-expressing lncRNA CASC15 (oe-CASC15), wt-CASC15, mut-CASC15, wt-MMP7, mut-MMP7 and relative NC plasmids alone or in combination. The aforementioned plasmids were purchased from Dharmacon, Inc. (Lafayette, CO, USA). After 48 h of transfection, the cells were subjected to subsequent experiments.

RNA isolation and quantification

Total RNA content was extracted from tissues and KYSE270 and EC109 cells using an RNeasy Mini Kit (Qiagen, Valencia, CA, USA). Next, the total RNA was reverse transcribed into complementary DNA (cDNA) (20 µL) using the Primescript™ RT reagent Kit (RR047A, Takara Bio Inc., Otsu, Shiga, Japan). Real time qPCR was performed with the help of a SYBR® Premix Ex Taq™ II reagent kit (RR420A, Takara Bio Inc., Otsu, Shiga, Japan) in an ABI7500 real-time quantitative PCR system (Applied Biosystems, Foster City, CA, USA). The primers used are listed in Table 2, which were synthesized by Shanghai Sangon Biotechnology Co., Ltd. (Shanghai, China).

Glyceraldehyde-3-phosphate dehydrogenase (GAPDH) or U6 was regarded as endogenous controls, and relative quantification (2^{-ΔΔC_t} method) was adopted to calculate the fold changes [59].

FISH

FISH technique was adopted to identify the subcellular localization of lncRNA CASC15 in the ESCC cells. EC109 cells were hybridized with several nucleotide probes against lncRNA CASC15 following the manufacturer's instructions for the Ribo™ lncRNA FISH Probe Mix (Red) (C10920, Guangzhou RiboBio Co., Ltd., Guangzhou, China). In brief, the cells were grown in 24-well plates until reaching 60 - 70% confluence. After fixation with 4% paraformaldehyde, the cells were permeabilized in phosphate-buffered saline (PBS) containing 0.5% Triton X-100 and blocked using 200 µL pre-hybridization solution at 37°C for 30 min. Cells were then incubated with the nucleotide probe against lncRNA CASC15 (Wuhan Genecreate Bioengineering Co., Ltd., Hubei, China) overnight at 37°C in conditions avoiding exposure to light. Next, the cells were stained using 4',6-diamidino-2-phenylindole (DAPI) and observed under a fluorescence microscope (Olympus Optical Co., Ltd., Tokyo, Japan) with 5 randomly selected fields from each sample.

RIP assay

RIP was conducted in the normal EC109 cells or those transfected with the plasmids of sh-CASC15 or oe-CASC15. EC109 cells were then lysed using 100 mL RIP lysis buffer (N653, Haoran Bio Technologies Co., Ltd., Shanghai, China) over ice for 5 min. Next, the cell lysate was added for incubation with 50 µL magnetic beads and 0.5 mL RIP wash buffer (EHJ-BVIS08102, Xiamen Huijia Biotechnology Co., Ltd., Fujian, China). After discarding the supernatant, the magnetic beads were incubated with 5 µg Argonaute 2 (AGO2) antibody (P10502500, Otwo Biotech Co., Ltd., Shenzhen, China) at room temperature for 30 min, with the normal mouse immunoglobulin G (IgG) serving as control. Subsequently, the antibody-coated magnetic beads were resuspended in 900 µL RIP Immunoprecipitation Buffer (P10403138, Otwo Biotech Co., Ltd., Shenzhen, China). After purification with 150 µL proteinase K buffer, RNA context was extracted from the magnetic beads using the Trizol reagent, followed by RT-qPCR detection. The experiment was performed in triplicate to obtain a mean value.

Western blot analysis

Total protein was extracted from the tissues and cells using radio-immunoprecipitation assay (RIPA) lysis

Table 2. Primer sequences for RT-qPCR.

Gene	Sequence
CASC15#1	F: 5'-TCATTCTTACCTCTTTCTCCAG-3'
	R:5'-CCCCCAATCACTTACTCTCTCT-3'
CASC15#2	F: 5'-CACACGCATGGAAAACCCAG-3'
	R: 5'-GAGGACCTGAGCTGTAAGCC-3'
CASC15#3	F: 5'-TGGAGTCCAAGTGTGACTGCCAAG-3'
	R: 5'-TCCTCTGGGTTTTCCATGCGTGT-3'
miR-140-5p	F: 5'-AGGTACCAGAACAAGCTAAGCAAAGG-3'
	R:5'-CAAGCTATGAAATCATCCCAACAAGC-3'
MMP7	F: 5'-GAGTGAGCTACAGTGGGAACA-3'
	R: 5'-CTATGACGGAGTTTAACAT-3'
MMP2	F: 5'-TTCCGCTTCCAGGGCACA-3'
	R: 5'-CACCTTCTGAGTTCCACCAA-3'
GAPDH	F: 5'-GGAGCGAGATCCCTCCAAT-3'
	R:5'-GGGCTGTTGTC AACTTCTCATGG-3'
U6	F:5'-CTCGCTTCGCAGCACATA-3'
	R:5'-GTGCAGGGTGAGCT-3'

Note: RT-qPCR, reverse transcription quantitative polymerase chain reaction; CASC15, cancer susceptibility 15; miR-140-5p, microRNA-140-5p; MMP7, matrix metalloproteinase 7; GAPDH, glyceraldehyde-3-phosphate dehydrogenase.

buffer containing phenylmethane sulfonyl fluoride (PMSF). After supernatant collection, a bicinchoninic acid (BCA) kit was employed to determine the protein concentration. A total of 50 µg of protein was separated by conducting sodium dodecyl sulfate-polyacrylamide gel electrophoresis (SDS-PAGE) and transferred onto a polyvinylidene fluoride membrane. Next, a membrane blockade was conducted using 5% skimmed milk at room temperature for 1 h and subjected to incubation with the diluted rabbit anti-human primary antibodies purchased from Abcam (Cambridge, UK) at 4° C overnight: GAPDH (as an internal control, ab9485, dilution ratio of 1 : 2,500), Fas (ab133619, dilution ratio of 1 : 5000), Ki-67 (ab92742, dilution ratio of 1 : 5,000), MMP7 (ab5706, dilution ratio of 1: 1000), and cleaved Caspase 3 (ab2302, dilution ratio of 1 : 1,000). Then, the membrane was incubated with the horseradish peroxidase (HRP)-labeled goat anti-rabbit IgG secondary antibody (ab97051, dilution ratio of 1 : 2000, Abcam company, Shanghai, China) for 1 h at 37° C. Subsequently, enhanced chemiluminescence (ECL) was adopted to visualize the bands using a Bio-Rad Gel

imager (Bio-Rad, Richmond, CA, USA). The gray value was measured using the Quantity One version 4.6.2 software, and the gray value ratio was calculated relative to the internal reference. The experiment was performed in triplicate in each group to obtain the mean value.

Dual-luciferase reporter assay

Luciferase reporter plasmids containing wt-CASC15, mut-CASC15, wt-MMP7, as well as mut-MMP7 were designed and constructed by GenePharma Co., Ltd., (Shanghai, China). The NC mimics and miR-140-5p mimics were respectively co-transfected with wt-CASC15, mut-CASC15, wt-MMP7 or mut-MMP7 plasmids and the renilla plasmid into EC109 cells. 48 h after transfection, a Dual-Luciferase Reporter Assay kit (D0010, Beijing Solarbio Science and Technology Co., Ltd. (Beijing, China) was employed to detect the firefly and renilla luciferase activities. The luminance was measured using a GLomax 20/20 Luminometer (E5311, Shaanxi Zhongmei Biotechnology Co., Ltd., Xi'an,

China). The experiment was performed in triplicate in each group to obtain the mean value.

CCK-8 assay for cell viability

Cells were inoculated in 96-well plates at a density of 2×10^3 cells/well. After 24 h of transfection, the cells were irradiated with X-ray at 4 Gy. Cells in each well were incubated with 10 μ L of CCK-8 solution at 37° C at 0, 24, 48, 72, and 96 h after irradiation, respectively. The absorbance of the samples was measured at an excitation wavelength of 450 nm using an enzyme labeling instrument (Bio-Rad, Hercules, CA, USA). The experiment was performed in triplicate in each group to obtain the mean value. The cell viability curve was then plotted based on the absorbance ratio of the experimental group relative to the blank control group.

Transwell assay for cell invasion

The upper chamber of the transwell filter chamber (40111ES08, Yeasen Company, Shanghai, China) was coated with diluted Matrigel (1 : 8 dilution in pre-cold serum-free DMEM) and incubated at 37° C for 4 - 5 h. The transfected cells were diluted using 100 μ L serum-free medium. Cell suspension (1×10^6 cells/mL) was then inoculated into the upper chamber of the transwell filter (in triplicate) and cultured for 24 h at 37° C with 5% CO₂ in air (addition of 500 μ L DMEM medium containing 20% FBS to the lower chamber). The invasive cells on the inferior chamber of the filter were fixed with 5% glutaraldehyde at 4° C, stained with 0.1% crystal violet, and observed under an inverted fluorescence microscope (TE2000, Nikon, Tokyo, Japan). Five fields in each transwell filter were selected randomly and photographed. The experiment was performed in triplicate to obtain the mean value of the number of the invasive cells in each group.

Flow cytometry for cell apoptosis

Cells were inoculated into 6-well plates at a density of 1×10^6 cells/well. After a 24 h period post-transfection, the cells were irradiated with X-ray at 4 Gy. Cells were collected 24 h after irradiation and cell apoptosis was detected using Annexin V-fluorescein isothiocyanate (FITC) and propidium iodide (PI) cell apoptosis kit (Invitrogen, Carlsbad, California, USA) with a FACSCalibur flow cytometer (BD Biosciences, San Jose, CA, USA). The experiment was performed in triplicate in each group to obtain the mean value.

Colony formation assay

A total of 1×10^3 cells at the logarithmic growth phase were inoculated in 6-well plates supplemented

with complete medium and cultured overnight. Cells were then exposed to 0, 2, 4, 6, and 8 Gy X-ray radiations at a dose of 3.5 Gy/min. After incubation at 37° C with 5% CO₂ in air for 14 d, the cells were fixed using methanol for 5 min and stained with crystal violet for 3 min. Colonies encompassing more than 50 cells were counted and documented under a microscope. Survival fraction (SF) = [the number of colonies with more than 50 cells / (the number of inoculated cells \times plating efficiency)] \times 100%, and the plating efficiency = the number of colonies / the number of inoculated cells were calculated. The experiment was performed in triplicate in each group to obtain the mean value.

Tumor xenografts in nude mice

A total of 24 female BALA/C nude mice (aged 4 weeks; weighing: 18 - 25 g) were obtained from the Animal Experimental Center of Zhengzhou University. The mice were then assigned into the sh-NC and sh-CASC15 groups and raised under specific pathogen-free conditions. Lentivirus containing shRNA against lncRNA CASC15 (LV-sh-CASC15) or scramble shRNA (LV-sh-NC) were purchased from GenePharma Co., Ltd., (Shanghai, China). A total of 1×10^6 EC109 cells soundly infected with lentivirus were subcutaneously injected into the right abdomen of the nude mice. Upon observing the mean volume of transplanted tumors as about 300 mm³, the mice were irradiated once a week using X-ray at 4 Gy. The volume of the transplanted tumors was measured regularly every three days after being subjected to irradiation. The volume of the transplanted tumor = $1/2 \times$ tumor length \times tumor width². Twenty-one days after the first irradiation, the nude mice were euthanized by carbon dioxide asphyxia and the tumors were excised for subsequent weighing and IHC analysis.

IHC analysis

Paraffin-embedded tissue slices were dewaxed using the conventional manner and subsequently underwent antigen retrieval under high pressure at 95° C in 0.01 M citric acid buffer (pH = 6.0) for 20 min. The slices were then immersed in 3% H₂O₂ for 15 min to terminate the peroxidase activity. After conducting a blockade using 3% bovine serum albumin (BSA), the slices were incubated with the rabbit anti-human Ki-67 (ab92742, dilution ratio of 1 : 500, Abcam, Cambridge, UK) or rabbit anti-human cleaved Caspase 3 (ab2302, dilution ratio of 1 : 200, Abcam, Cambridge, UK) at 37° C for 2 h. After an additional PBS rinse, the slices were incubated with the HRP-labeled goat anti-rabbit IgG secondary antibody (Abcam, Cambridge, UK) in a wet box for 30 min at

37° C. The slices were then counter-stained with hematoxylin (Shanghai Fusheng Industrial Co., Ltd., Shanghai, China), washed under running water, and mounted with 10% glycerol/PBS. The experiment was performed in triplicate and the results were evaluated and scored by two individuals independently.

Statistical analysis

All experimental data were processed and analyzed using the Statistic Package for Social Science (SPSS) 22.0 statistical software (IBM Corp. Armonk, NY, USA). Measurement data are presented as mean \pm standard deviation. Differences between two groups were analyzed by unpaired *t* test or paired *t* test. Comparisons among multiple groups were analyzed using one-way analysis of variance (ANOVA), followed by Tukey's post-hoc test. Tumor volumes between the groups were compared using repeated-measures ANOVA. Pearson correlation analysis was adopted to verify the correlations between the expression of lncRNA CASC15 and miR-140-5p or MMP7 in ESCC tissues, and Kaplan-Meier analysis with the log-rank test was performed to assess the survival time of patients with aberrant lncRNA CASC15 expression. A value of $p < 0.05$ was considered to be statistically significant.

AUTHOR CONTRIBUTIONS

Chengliang Yang, Yufeng Ba and Xiaoli Zheng designed the study. Ke Ye, Hong Ge and Yanan Sun collated the data, carried out data analyses and produced the initial draft of the manuscript. Chengliang Yang, Yufeng Ba, Yanan Sun and Yufei Lu contributed to drafting the manuscript. All authors have read and approved the final submitted manuscript.

ACKNOWLEDGMENTS

The authors express sincere appreciation to the reviewers for critical comments on this article.

CONFLICTS OF INTEREST

The authors declare that they have no conflicts of interest.

REFERENCES

1. Zhang Y. Epidemiology of esophageal cancer. *World J Gastroenterol.* 2013; 19:5598–606.
<https://doi.org/10.3748/wjg.v19.i34.5598>
PMID:24039351
2. Napier KJ, Scheerer M, Misra S. Esophageal cancer: A Review of epidemiology, pathogenesis, staging workup and treatment modalities. *World J Gastrointest Oncol.* 2014; 6:112–20.
<https://doi.org/10.4251/wjgo.v6.i5.112>
PMID:24834141
3. Arnold M, Soerjomataram I, Ferlay J, Forman D. Global incidence of oesophageal cancer by histological subtype in 2012. *Gut.* 2015; 64:381–87.
<https://doi.org/10.2188/jea.JE20120162>
PMID:25320104
4. Lin Y, Totsuka Y, He Y, Kikuchi S, Qiao Y, Ueda J, Wei W, Inoue M, Tanaka H. Epidemiology of esophageal cancer in Japan and China. *J Epidemiol.* 2013; 23:233–42.
<https://doi.org/10.2188/jea.je20120162>
PMID:23629646
5. Castro C, Peleteiro B, Lunet N. Modifiable factors and esophageal cancer: a systematic review of published meta-analyses. *J Gastroenterol.* 2018; 53:37–51.
<https://doi.org/10.1007/s00535-017-1375-5>
PMID:28821981
6. Siosaki MD, Lacerda CF, Bertulucci PA, da Costa Filho JO, de Oliveira AT. Bypass laparoscopic procedure for palliation of esophageal cancer. *J Surg Case Rep.* 2013; 2013:rjt017.
<https://doi.org/10.1093/jscr/rjt017>
PMID:24964427
7. Ilson DH, van Hillegersberg R. Management of patients with adenocarcinoma or squamous cancer of the esophagus. *Gastroenterology.* 2018; 154:437–51.
<https://doi.org/10.1053/j.gastro.2017.09.048>
PMID:29037469
8. Markar S, Gronnier C, Duhamel A, Pasquer A, Théreaux J, du Rieu MC, Lefevre JH, Turner K, Luc G, Mariette C. Salvage surgery after chemoradiotherapy in the management of esophageal cancer: is it a viable therapeutic option? *J Clin Oncol.* 2015; 33:3866–73.
<https://doi.org/10.1200/JCO.2014.59.9092>
PMID:26195702
9. Backemar L, Lagergren P, Djärv T, Johar A, Wikman A, Lagergren J. Comorbidities and risk of complications after surgery for esophageal cancer: a nationwide cohort study in Sweden. *World J Surg.* 2015; 39:2282–88.
<https://doi.org/10.1007/s00268-015-3093-6>
PMID:25952691
10. Chen GZ, Zhu HC, Dai WS, Zeng XN, Luo JH, Sun XC. The mechanisms of radioresistance in esophageal squamous cell carcinoma and current strategies in radiosensitivity. *J Thorac Dis.* 2017; 9:849–59.
<https://doi.org/10.21037/jtd.2017.03.23>
PMID:28449496
11. Zhang H, Luo H, Jiang Z, Yue J, Hou Q, Xie R, Wu S. Fractionated irradiation-induced EMT-like phenotype

- conferred radioresistance in esophageal squamous cell carcinoma. *J Radiat Res.* 2016; 57:370–80.
<https://doi.org/10.1093/jrr/rrw030>
 PMID:27125498
12. Evans JR, Feng FY, Chinnaiyan AM. The bright side of dark matter: lncRNAs in cancer. *J Clin Invest.* 2016; 126:2775–82.
<https://doi.org/10.1172/JCI84421> PMID:27479746
 13. Schmitt AM, Chang HY. Long noncoding RNAs in cancer pathways. *Cancer Cell.* 2016; 29:452–63.
<https://doi.org/10.1016/j.ccell.2016.03.010>
 PMID:27070700
 14. Huang X, Zhou X, Hu Q, Sun B, Deng M, Qi X, Lü M. Advances in esophageal cancer: A new perspective on pathogenesis associated with long non-coding RNAs. *Cancer Lett.* 2018; 413:94–101.
<https://doi.org/10.1016/j.canlet.2017.10.046>
 PMID:29104147
 15. Capasso M, Diskin SJ, Totaro F, Longo L, De Mariano M, Russo R, Cimmino F, Hakonarson H, Tonini GP, Devoto M, Maris JM, Iolascon A. Replication of GWAS-identified neuroblastoma risk loci strengthens the role of BARD1 and affirms the cumulative effect of genetic variations on disease susceptibility. *Carcinogenesis.* 2013; 34:605–11.
<https://doi.org/10.1093/carcin/bgs380>
 PMID:23222812
 16. Yao XM, Tang JH, Zhu H, Jing Y. High expression of lncRNA CASC15 is a risk factor for gastric cancer prognosis and promote the proliferation of gastric cancer. *Eur Rev Med Pharmacol Sci.* 2017; 21:5661–67.
https://doi.org/10.26355/eurrev_201712_14010
 PMID:29272000
 17. He T, Zhang L, Kong Y, Huang Y, Zhang Y, Zhou D, Zhou X, Yan Y, Zhang L, Lu S, Zhou J, Wang W. Long non-coding RNA CASC15 is upregulated in hepatocellular carcinoma and facilitates hepatocarcinogenesis. *Int J Oncol.* 2017; 51:1722–30.
<https://doi.org/10.3892/ijo.2017.4175>
 PMID:29075788
 18. Wang W, Wei C, Li P, Wang L, Li W, Chen K, Zhang J, Zhang W, Jiang G. Integrative analysis of mRNA and lncRNA profiles identified pathogenetic lncRNAs in esophageal squamous cell carcinoma. *Gene.* 2018; 661:169–75.
<https://doi.org/10.1016/j.gene.2018.03.066>
 PMID:29604464
 19. Malhotra A, Sharma U, Puhan S, Chandra Bandari N, Kharb A, Arifa PP, Thakur L, Prakash H, Vasquez KM, Jain A. Stabilization of miRNAs in esophageal cancer contributes to radioresistance and limits efficacy of therapy. *Biochimie.* 2019; 156:148–57.
<https://doi.org/10.1016/j.biochi.2018.10.006>
 PMID:30326253
 20. Fang Z, Yin S, Sun R, Zhang S, Fu M, Wu Y, Zhang T, Khaliq J, Li Y. miR-140-5p suppresses the proliferation, migration and invasion of gastric cancer by regulating YES1. *Mol Cancer.* 2017; 16:139.
<https://doi.org/10.1186/s12943-017-0708-6>
 PMID:28818100
 21. Peng YP, Zhu Y, Yin LD, Zhang JJ, Guo S, Fu Y, Miao Y, Wei JS. The expression and prognostic roles of MCMs in pancreatic cancer. *PLoS One.* 2016; 11:e0164150.
<https://doi.org/10.1371/journal.pone.0164150>
 PMID:27695057
 22. Miao S, Zhou SY, Han CS, Zhang LN, Sun HB, Yang B. Clinicopathological significance of matrix metalloproteinase-7 protein expression in esophageal cancer: a meta-analysis. *Drug Des Devel Ther.* 2015; 9:3729–40.
<https://doi.org/10.2147/DDDT.S85987>
 PMID:26229436
 23. Zhang W, Li Y, Yang L, Zhou B, Chen KL, Meng WJ, Liu Y, Hu JK, Sun XF, Zhou ZG. Knockdown of MMP-7 inhibits cell proliferation and enhances sensitivity to 5-Fluorouracil and X-ray irradiation in colon cancer cells. *Clin Exp Med.* 2014; 14:99–106.
<https://doi.org/10.1007/s10238-012-0212-7>
 PMID:23086188
 24. Juchniewicz A, Kowalczyk O, Milewski R, Ludański W, Dzięgielewski P, Kozłowski M, Nikliński J. MMP-10, MMP-7, TIMP-1 and TIMP-2 mRNA expression in esophageal cancer. *Acta Biochim Pol.* 2017; 64:295–99.
https://doi.org/10.18388/abp.2016_1408
 PMID:28510611
 25. Long ZW, Wang JL, Wang YN. Matrix metalloproteinase-7 mRNA and protein expression in gastric carcinoma: a meta-analysis. *Tumour Biol.* 2014; 35:11415–26.
<https://doi.org/10.1007/s13277-014-2441-8>
 PMID:25123263
 26. Zhou JH, Zhang B, Kernstine KH, Zhong L. Autoantibodies against MMP-7 as a novel diagnostic biomarker in esophageal squamous cell carcinoma. *World J Gastroenterol.* 2011; 17:1373–78.
<https://doi.org/10.3748/wjg.v17.i10.1373>
 PMID:21455340
 27. Stene C, Polistena A, Gaber A, Nodin B, Ottochian B, Adawi D, Avenia N, Jirstrom K, Johnson LB. MMP7 modulation by short- and long-term radiotherapy in patients with rectal cancer. *In Vivo.* 2018; 32:133–38.
<https://doi.org/10.21873/invivo.11215>
 PMID:29275310

28. Singh A, Singh A, Bauer SJ, Wheeler DL, Havighurst TC, Kim K, Verma AK. Genetic deletion of TNF α inhibits ultraviolet radiation-induced development of cutaneous squamous cell carcinomas in PKC ϵ transgenic mice via inhibition of cell survival signals. *Carcinogenesis*. 2016; 37:72–80.
<https://doi.org/10.1093/carcin/bgv162>
PMID:[26586792](https://pubmed.ncbi.nlm.nih.gov/26586792/)
29. Liang H, Fan JH, Qiao YL. Epidemiology, etiology, and prevention of esophageal squamous cell carcinoma in China. *Cancer Biol Med*. 2017; 14:33–41.
<https://doi.org/10.20892/j.issn.2095-3941.2016.0093>
PMID:[28443201](https://pubmed.ncbi.nlm.nih.gov/28443201/)
30. Lessard L, Liu M, Marzese DM, Wang H, Chong K, Kawas N, Donovan NC, Kiyohara E, Hsu S, Nelson N, Izraely S, Sagi-Assif O, Witz IP, et al. The CASC15 long intergenic noncoding RNA locus is involved in melanoma progression and phenotype switching. *J Invest Dermatol*. 2015; 135:2464–74.
<https://doi.org/10.1038/jid.2015.200>
PMID:[26016895](https://pubmed.ncbi.nlm.nih.gov/26016895/)
31. Fernando TR, Contreras JR, Zampini M, Rodriguez-Malave NI, Alberti MO, Anguiano J, Tran TM, Palanichamy JK, Gajeton J, Ung NM, Aros CJ, Waters EV, Casero D, et al. The lncRNA CASC15 regulates SOX4 expression in RUNX1-rearranged acute leukemia. *Mol Cancer*. 2017; 16:126.
<https://doi.org/10.1186/s12943-017-0692-x>
PMID:[28724437](https://pubmed.ncbi.nlm.nih.gov/28724437/)
32. Zuo Z, Ma L, Gong Z, Xue L, Wang Q. Long non-coding RNA CASC15 promotes tongue squamous carcinoma progression through targeting miR-33a-5p. *Environ Sci Pollut Res Int*. 2018; 25:22205–12.
<https://doi.org/10.1007/s11356-018-2300-z>
PMID:[29804249](https://pubmed.ncbi.nlm.nih.gov/29804249/)
33. Shen WJ, Zhang F, Zhao X, Xu J. LncRNAs and esophageal squamous cell carcinoma - implications for pathogenesis and drug development. *J Cancer*. 2016; 7:1258–64.
<https://doi.org/10.7150/jca.14869>
PMID:[27390601](https://pubmed.ncbi.nlm.nih.gov/27390601/)
34. Hang Q, Sun R, Jiang C, Li Y. Notch 1 promotes cisplatin-resistant gastric cancer formation by upregulating lncRNA AK022798 expression. *Anticancer Drugs*. 2015; 26:632–40.
<https://doi.org/10.1097/CAD.0000000000000227>
PMID:[25763542](https://pubmed.ncbi.nlm.nih.gov/25763542/)
35. Yan J, Dang Y, Liu S, Zhang Y, Zhang G. LncRNA HOTAIR promotes cisplatin resistance in gastric cancer by targeting miR-126 to activate the PI3K/AKT/MRP1 genes. *Tumour Biol*. 2016. [Epub ahead of print].
<https://doi.org/10.1007/s13277-016-5448-5>
PMID:[27900563](https://pubmed.ncbi.nlm.nih.gov/27900563/)
36. Fu HL, Wu DP, Wang XF, Wang JG, Jiao F, Song LL, Xie H, Wen XY, Shan HS, Du YX, Zhao YP. Altered miRNA expression is associated with differentiation, invasion, and metastasis of esophageal squamous cell carcinoma (ESCC) in patients from Huaian, China. *Cell Biochem Biophys*. 2013; 67:657–68.
<https://doi.org/10.1007/s12013-013-9554-3>
PMID:[23516093](https://pubmed.ncbi.nlm.nih.gov/23516093/)
37. Hui B, Chen X, Hui L, Xi R, Zhang X. Serum miRNA expression in patients with esophageal squamous cell carcinoma. *Oncol Lett*. 2015; 10:3008–12.
<https://doi.org/10.3892/ol.2015.3642> PMID:[26722280](https://pubmed.ncbi.nlm.nih.gov/26722280/)
38. Lin RJ, Xiao DW, Liao LD, Chen T, Xie ZF, Huang WZ, Wang WS, Jiang TF, Wu BL, Li EM, Xu LY. MiR-142-3p as a potential prognostic biomarker for esophageal squamous cell carcinoma. *J Surg Oncol*. 2012; 105:175–82.
<https://doi.org/10.1002/jso.22066>
PMID:[21882196](https://pubmed.ncbi.nlm.nih.gov/21882196/)
39. Mayne GC, Hussey DJ, Watson DI. MicroRNAs and esophageal cancer—implications for pathogenesis and therapy. *Curr Pharm Des*. 2013; 19:1211–26.
<https://doi.org/10.2174/138161213804805702>
PMID:[23092342](https://pubmed.ncbi.nlm.nih.gov/23092342/)
40. Liu J, Li M, Wang Y, Luo J. Curcumin sensitizes prostate cancer cells to radiation partly via epigenetic activation of miR-143 and miR-143 mediated autophagy inhibition. *J Drug Target*. 2017; 25:645–52.
<https://doi.org/10.1080/1061186X.2017.1315686>
PMID:[28391715](https://pubmed.ncbi.nlm.nih.gov/28391715/)
41. Zhang K, Chen J, Song H, Chen LB. SNHG16/miR-140-5p axis promotes esophagus cancer cell proliferation, migration and EMT formation through regulating ZEB1. *Oncotarget*. 2017; 9:1028–40.
<https://doi.org/10.18632/oncotarget.23178>
PMID:[29416674](https://pubmed.ncbi.nlm.nih.gov/29416674/)
42. Yuan S, Lin LS, Gan RH, Huang L, Wu XT, Zhao Y, Su BH, Zheng D, Lu YG. Elevated matrix metalloproteinase 7 expression promotes the proliferation, motility and metastasis of tongue squamous cell carcinoma. *BMC Cancer*. 2020; 20:33.
<https://doi.org/10.1186/s12885-020-6521-4>
PMID:[31937294](https://pubmed.ncbi.nlm.nih.gov/31937294/)
43. Liu H, Zhang T, Li X, Huang J, Wu B, Huang X, Zhou Y, Zhu J, Hou J. Predictive value of MMP-7 expression for response to chemotherapy and survival in patients with non-small cell lung cancer. *Cancer Sci*. 2008; 99:2185–92.
<https://doi.org/10.1111/j.1349-7006.2008.00922.x>
PMID:[18823373](https://pubmed.ncbi.nlm.nih.gov/18823373/)
44. Huang Y, Yu H, Lei H, Xie C, Zhong Y. Matrix metalloproteinase 7 is a useful marker for 5-

- fluorouracil-based adjuvant chemotherapy in stage II and stage III colorectal cancer patients. *Med Oncol*. 2014; 31:824.
<https://doi.org/10.1007/s12032-013-0824-0>
PMID:[24469951](https://pubmed.ncbi.nlm.nih.gov/24469951/)
45. Almendro V, Ametller E, García-Recio S, Collazo O, Casas I, Augé JM, Maurel J, Gascón P. The role of MMP7 and its cross-talk with the FAS/FASL system during the acquisition of chemoresistance to oxaliplatin. *PLoS One*. 2009; 4:e4728.
<https://doi.org/10.1371/journal.pone.0004728>
PMID:[19266094](https://pubmed.ncbi.nlm.nih.gov/19266094/)
46. Alla V, Kashyap A, Gregor S, Theobald M, Heid H, Galle PR, Strand D, Strand S. Human leukocyte elastase counteracts matrix metalloproteinase-7 induced apoptosis resistance of tumor cells. *Cancer Lett*. 2008; 268:331–39.
<https://doi.org/10.1016/j.canlet.2008.04.006>
PMID:[18485588](https://pubmed.ncbi.nlm.nih.gov/18485588/)
47. Nishioka M, Shimada M, Kurita N, Iwata T, Morimoto S, Yoshikawa K, Higashijima J, Miyatani T. Gene expression profile can predict pathological response to preoperative chemoradiotherapy in rectal cancer. *Cancer Genomics Proteomics*. 2011; 8:87–92.
PMID:[21471518](https://pubmed.ncbi.nlm.nih.gov/21471518/)
48. Abba M, Patil N, Allgayer H. MicroRNAs in the regulation of MMPs and metastasis. *Cancers (Basel)*. 2014; 6:625–45.
<https://doi.org/10.3390/cancers6020625>
PMID:[24670365](https://pubmed.ncbi.nlm.nih.gov/24670365/)
49. Yang L, Song X, Zhu J, Li M, Ji Y, Wu F, Chen Y, Cui X, Hu J, Wang L, Cao Y, Wei Y, Zhang W, Li F. Tumor suppressor microRNA-34a inhibits cell migration and invasion by targeting MMP-2/MMP-9/FNDC3B in esophageal squamous cell carcinoma. *Int J Oncol*. 2017; 51:378–88.
<https://doi.org/10.3892/ijo.2017.4015> PMID:[28534990](https://pubmed.ncbi.nlm.nih.gov/28534990/)
50. Osako Y, Seki N, Kita Y, Yonemori K, Koshizuka K, Kurozumi A, Omoto I, Sasaki K, Uchikado Y, Kurahara H, Maemura K, Natsugoe S. Regulation of MMP13 by antitumor microRNA-375 markedly inhibits cancer cell migration and invasion in esophageal squamous cell carcinoma. *Int J Oncol*. 2016; 49:2255–64.
<https://doi.org/10.3892/ijo.2016.3745>
PMID:[27779648](https://pubmed.ncbi.nlm.nih.gov/27779648/)
51. Wu D, Huang P, Wang L, Zhou Y, Pan H, Qu P. MicroRNA-143 inhibits cell migration and invasion by targeting matrix metalloproteinase 13 in prostate cancer. *Mol Med Rep*. 2013; 8:626–30.
<https://doi.org/10.3892/mmr.2013.1501>
PMID:[23732700](https://pubmed.ncbi.nlm.nih.gov/23732700/)
52. Wang XY, Jensen-Taubman SM, Keefe KM, Yang D, Linnoila RI. Achaete-scute complex homolog-1 promotes DNA repair in the lung carcinogenesis through matrix metalloproteinase-7 and O(6)-methylguanine-DNA methyltransferase. *PLoS One*. 2012; 7:e52832.
<https://doi.org/10.1371/journal.pone.0052832>
PMID:[23300791](https://pubmed.ncbi.nlm.nih.gov/23300791/)
53. Daniel AG, Peterson EJ, Farrell NP. The bioinorganic chemistry of apoptosis: potential inhibitory zinc binding sites in caspase-3. *Angew Chem Int Ed Engl*. 2014; 53:4098–101.
<https://doi.org/10.1002/anie.201311114>
PMID:[24643997](https://pubmed.ncbi.nlm.nih.gov/24643997/)
54. Chierico L, Rizzello L, Guan L, Joseph AS, Lewis A, Battaglia G. The role of the two splice variants and extranuclear pathway on Ki-67 regulation in non-cancer and cancer cells. *PLoS One*. 2017; 12:e0171815.
<https://doi.org/10.1371/journal.pone.0171815>
PMID:[28187152](https://pubmed.ncbi.nlm.nih.gov/28187152/)
55. Koo TR, Eom KY, Kang EY, Kim YJ, Kim SW, Kim JH, Kim JS, Kim IA. Prognostic value of the nodal ratio and ki-67 expression in breast cancer patients treated with postmastectomy radiotherapy. *J Breast Cancer*. 2013; 16:274–84.
<https://doi.org/10.4048/jbc.2013.16.3.274>
PMID:[24155756](https://pubmed.ncbi.nlm.nih.gov/24155756/)
56. Liu PF, Hu YC, Kang BH, Tseng YK, Wu PC, Liang CC, Hou YY, Fu TY, Liou HH, Hsieh IC, Ger LP, Shu CW. Expression levels of cleaved caspase-3 and caspase-3 in tumorigenesis and prognosis of oral tongue squamous cell carcinoma. *PLoS One*. 2017; 12:e0180620.
<https://doi.org/10.1371/journal.pone.0180620>
PMID:[28700659](https://pubmed.ncbi.nlm.nih.gov/28700659/)
57. Di Z, Sanyuan S, Hong L, Dahai Y. Enhanced radiosensitivity and G2/M arrest were observed in radioresistant esophageal cancer cells by knocking down RPA expression. *Cell Biochem Biophys*. 2014; 70:887–91.
<https://doi.org/10.1007/s12013-014-9995-3>
PMID:[24789547](https://pubmed.ncbi.nlm.nih.gov/24789547/)
58. Luo A, Zhou X, Shi X, Zhao Y, Men Y, Chang X, Chen H, Ding F, Li Y, Su D, Xiao Z, Hui Z, Liu Z. Exosome-derived miR-339-5p mediates radiosensitivity by targeting Cdc25A in locally advanced esophageal squamous cell carcinoma. *Oncogene*. 2019; 38:4990–5006.
<https://doi.org/10.1038/s41388-019-0771-0>
PMID:[30858545](https://pubmed.ncbi.nlm.nih.gov/30858545/)
59. Kok MG, Halliani A, Moerland PD, Meijers JC, Creemers EE, Pinto-Sietsma SJ. Normalization panels for the reliable quantification of circulating microRNAs by RT-qPCR. *FASEB J*. 2015; 29:3853–62.
<https://doi.org/10.1096/fj.15-271312>
PMID:[26023181](https://pubmed.ncbi.nlm.nih.gov/26023181/)